Development of biodegradable nanoparticle-based therapies against tuberculosis in a zebrafish model

Working towards the encapsulation of antimicrobial agents and peptide-encoding DNA

Marie Paulsen Madsen

Thesis for the Master's degree in Molecular Biosciences
60 study points

Department of Molecular Biosciences
Faculty of Mathematics and Natural Sciences

UNIVERSITY OF OSLO

September 2012

Acknowledgements

First and foremost, I have to thank my supervisor Prof. Gareth Griffiths for introducing me to the world of science and for his never-ending enthusiasm. I also need to thank former and present members of our group; David, Lilia, Urska, Arturas, Federico, Jon, Raja, Martin and Bård for always taking the time to help me in any way they can and answering all my questions.

Specifically, I want to give thanks to David for his guidance in the beginning of my Master's, and to Lilia and Urska for helping me with electron microscopy. Also, thanks needs to be given to Arturas for helping me with infection of adult zebrafish, and to Monica, who shared her knowledge in using PicoGreen with me.

I would also like to mention all the great people associated with the Gareth Griffiths group that I have gotten to know these past two years, from IMBV, the School of Veterinary Science, School of Pharmacy and the Chemistry Department, for creating such a fun and inspiring environment.

Finally, I want to thank my parents for always supporting and believing in me.

Marie Paulsen Madsen

Oslo, September 2012

Abstract

At the moment, one-third of the world's population is estimated to be infected with *Mycobacterium tuberculosis* (*M.tb*), the causative agent of tuberculosis (TB) in humans. Our treatment strategies have been greatly challenged due to the lack of an effective vaccine and the increasing emergence of drug-resistant strains. Following the lead of Gopal Khuller, we set out to elucidate a novel drug delivery system based on biodegradable nanoparticles (NPs). NPs loaded with anti-mycobacterial drugs, such as rifampicin (RIF), can be used to more effectively deliver drugs to the site of infection. In addition, these NPs facilitate sustained release and therefore, drastically decrease the number of doses needed during a typical treatment regimen. In this thesis, work towards the improvement of TB therapy was executed in two separate ways. First, using the *Mycobacterium marinum* (*M.marinum*)-zebrafish model system established by the group of Lalita Ramakrishnan, we evaluated the effects of the antibiotic, RIF, and the anti-mycobacterial compound that blocks bacterial efflux pumps, thioridazine (TZ), free in solution. This was accomplished with the use of drug baths; water supplemented with the bactericidal agent. With this method the morphological effects could readily be observed, and due to the transparency of zebrafish embryos, the fluorescent *M.marinum* bacilli could be visualized *in vivo*. Second, we were interested in using antimicrobial peptides to treat mycobacterial infections, as an alternative to antibiotics. Due to the already successful production of NPs loaded with RIF in our group, we sought to encapsulate plasmid DNA (pDNA) encoding these antimicrobial peptides using the nanoprecipitation method. The effects of different concentrations of RIF and TZ were observed in infected and uninfected zebrafish embryos. The infecting bacteria readily acquired tolerance towards RIF, as has been shown by others, but higher concentrations were found to show higher bactericidal activity and no observable toxicity. TZ is believed to increase the effects of antibiotics, such as RIF, and therefore eliminate the transient phenomenon of tolerance, but these effects were not observed under the conditions of the preliminary experiment performed here. Although pDNA encapsulation was not successful, NPs were fabricated in a narrow size range and protocols for preparation of NPs and for the analyses of pDNA integrity and loading were established. These protocols provide the foundation for others in our group to continue the further development of this promising NP-based therapy.

Table of contents

Abbreviations

ADC	Albumin, dextrose, catalase agar supplement
BCG	Bacille Calmette Guerin
CFP-10	10 kDa culture filtrate protein
Ci-MAM-A24	*Ciona*-molecule against microbes, 24 aa
CFU	Colony forming units
DMSO	Dimethyl sulfoxide
DNA	Deoxyribonucleic acid
dpf	Days post fertilization
dpi	Days post infection
dsDNA	Double-stranded DNA
EDTA	Ethylenediaminetetraacetic acid
EEA1	Early endosome antigen 1
EMBL	European Molecular Biology Laboratory
ESAT-6	6 kDa early secretory antigenic target
FCS	Fetal calf serum
GFP	Green fluorescent protein
HBD	Human β-defensin
hCAP18	Human cationic antimicrobial protein 18
HIV	Human immunodeficiency virus
HNP	Human neutrophil peptide
hpf	Hours post fertilization
HPLC	High-performance liquid chromatography
LAMP1	Lysosomal-associated membrane protein 1
MDR-TB	Multidrug-resistant TB
MEC	Minimum effective concentration
MeCN	Acetonitrile
MIC	Minimum inhibitory concentration
M.marinum	*Mycobacterium marinum*

mRNA	Messenger RNA
MRSA	Methicillin-resistant *Staphylococcus aureus*
M.tb	*Mycobacterium tuberculosis*
NK	Natural killer
NP	Nanoparticles
OD	Optical density
PBS	Phosphate buffered saline, pH 7.4
PCR	Polymerase chain reaction
pDNA	Plasmid DNA
PEG	Polyethylene glycol
PEI	Polyethyleneimine
PFA	Paraformaldahyde
PLGA	Poly(lactic-co-glycolic acid)
PVP	Polyvinylpyrrolidone
RD1	Region of difference 1
RIF	Rifampicin
RNA	Ribonucleic acid
rpm	Revolutions per minute
rRNA	Ribosomal RNA
TB	Tuberculosis
TDR	Totally drug-resistant
TEM	Transmission electron microscopy
TLR	Toll-like receptor
TZ	Thioridazine
WT	Wild type
XDR-TB	Extensively drug-resistant TB

1 Introduction

1.1 The burden of tuberculosis

The infectious agent responsible for the most deaths in the world today is *Mycobacterium tuberculosis (M.tb)*, the bacterial pathogen that causes tuberculosis (TB) in humans. In 2010, 8.8 million people were infected with tuberculosis and 1.4 million died from the disease, meaning 3,800 people died every day. In addition, 350,000 HIV positive individuals died from TB the same year. [1]

The most disturbing part may be the fact that at this moment, one-third of the world's population is infected with *M.tb* but due to latency, only a small proportion of these individuals actually become sick. Approximately 10 % of latently infected individuals will eventually progress to clinical disease [2]. This is common when the individual is in an immune-compromised state, such as old age, malnutrition, or due to HIV co-infection [3]. Despite these data, the number of TB infections has been declining since 2005, slowly but still declining. In 2009, 87 % of patients were successfully treated for TB, the highest rate ever [1].

Although we seem to be moving in the right direction, approximately 440,000 multidrug-resistant TB (MDR-TB) cases are estimated to emerge every year, and 150,000 people with MDR-TB will die as a consequence of it. MDR-TB bacteria are characterized by their resistance towards the first-line drugs isoniazid and rifampicin. The bacteria either acquire this resistance during treatment of TB or they have already acquired it upon primary infection. Unfortunately, in addition to MDR-TB, we also have the emergence of extensively drug-resistant TB (XDR-TB), which in addition to isoniazid and rifampicin, is also resistant to fluoroquinolone and any of the injectable second-line anti-TB drugs [4], such as kanamycin. Finally, even totally drug-resistant (TDR) strains have recently been uncovered, which are characterized as MDR strains also resistant to all second-line drug classes [5].

The drugs we have today are effective against TB, but the current treatment regimen requires more than 6 months and consists of a cocktail of these drugs. When dealing with drug-resistant strains, treatment can take more than 2 years and requires the use of less potent drugs, which are more toxic and more expensive [4]. This treatment regimen leads to issues

of patient non-compliance, inadequate health-care oversight, and of course, an increasing number of resistant strains [6].

Therefore, it is safe to say, the need for more effective treatments is immediate and compelling.

1.1.1 Life cycle of *Mycobacterium tuberculosis*

*M.tb*s route of infection is invariably through the inhalation of airborne bacilli and a single bacterium may be enough to initiate an infection [6].
As depicted in Figure 1: after *M.tb* reaches the alveolar space of the human lung the bacterium is phagocytosed by alveolar macrophages, which facilitate invasion of the epithelial layer in the human lung. Macrophages do not kill the bacterium but, along with dendritic cells, carry the bacterium to draining lymph nodes. An inflammatory response is then initiated and mononuclear cells are recruited to the site of infection.

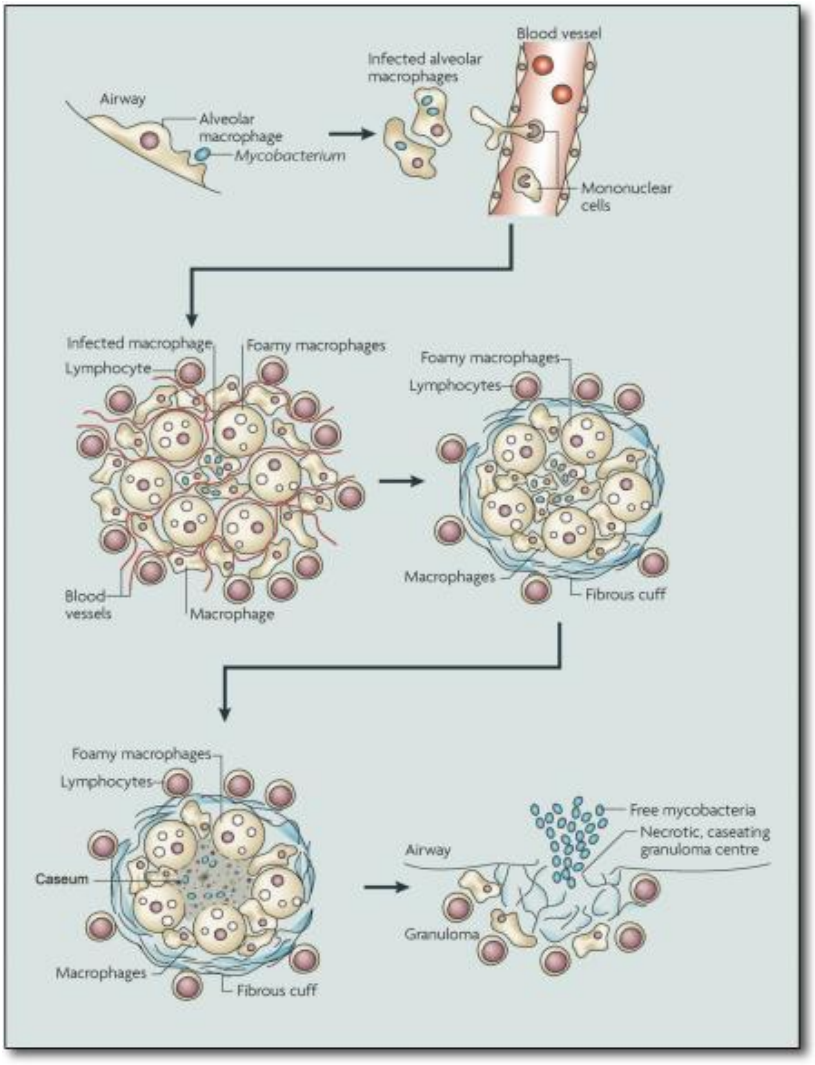

Figure 1: Infection cycle of *M.tb*. Starting in the alveolar space, this figure depicts the sequence of events following infection of *M.tb*. Figure from Russell et al., 2010 **[6]**

The recruited cells will take part in the building of the granuloma (organized aggregates of immune cells) and the expansion of the bacterial population. The infected macrophages will then differentiate into several specialized cells, including foamy and epithelioid macrophages, which will create the core of the granuloma. Eventually, an acquired immune response will lead to lymphocytes surrounding the macrophage core in association with a fibrous cuff made of extracellular matrix, making up the periphery of the granuloma [6].
This phase is typically called the "containment" phase, where the host shows no sign of disease, and is not contagious. If a change occurs in the host's immune status, such as a decrease, or increase in pro-inflammatory or anti-inflammatory responses, the center of the granuloma undergoes caseation and spills infectious bacilli into the airways. This leads to the host coughing and subsequent spread of the bacilli to new hosts [3].

In humans, the tuberculous granuloma is a highly organized structure that represents a balance between host and pathogen. For the host, the granuloma provides a focal point for the immune response. It serves to some degree for containment of the infection and, thereby, hopes to limit bacterial dissemination. For the pathogen, the pro-inflammatory environment of the granuloma recruits potential host cells and maintains lymphocytes at the periphery of the structure, where macrophage activation is likely to be less effective [7].

1.1.2 How does *Mycobacterium tuberculosis* survive inside macrophages?

Many different kinds of macrophages are able to phagocytose *M.tb.* One major route of uptake for mycobacteria upon contact with macrophages is through complement receptors and complement opsonization, (the binding of complement factors to the bacteria) [8]. In addition, other receptors have been implicated, including mannose receptors, Toll-like receptors 2 and 4, surfactant protein A receptors, CD14, and scavenger receptors [9].
After uptake into macrophages, the mycobacteria-containing phagosome does not follow the normal phagosomal maturation pathway. Sequential fusion with early and late endosomes, and finally lysosomes, creates an increasingly more acidic and acid hydrolase-rich environment, eventually leading to the destruction of the bacteria. Rather, phagosome maturation is arrested in an early maturation state, where the phagosome fails to fuse with lysosomes.
Via et al. 1997 have shown that mycobacteria arrest phagosome maturation between the

stages marked by the regulatory GTPase Rab5 (an early endosome marker) and Rab7 (a late endosome and lysosome marker). They showed that Rab7 never associates with the mycobacterium-containing compartment, indicating the failure to fuse with lysosomes and, therefore, the successful blockage of phagosome maturation [10]. (Figure 2)

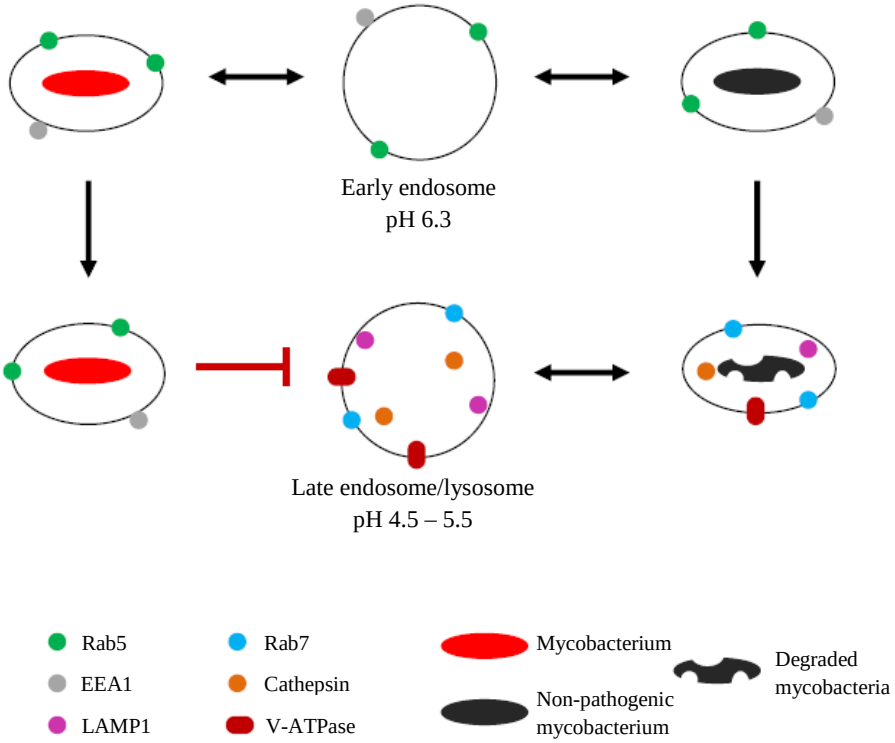

Figure 2: Phagosomal maturation pathway with pathogenic (left) and non-pathogenic (right) mycobacteria. Pathogenic mycobacteria have the ability to inhibit the fusion of late endosomes and lysosomes to the phagosomal compartment in which they reside, and therefore escape degradation by acid hydrolases, such as cathepsins. Rab5 and EEA1 (early endosome antigen 1) mark the early endosomal compartments. Rab7, LAMP1 (lysosomal-associated membrane protein 1), cathepsins and V-ATPases mark the late endosomal and lysosomal compartments.

It is believed that the pathogen blocks Ca^{2+} fluxes, which through subsequent steps, leads to a block in the fusion with lysosomes [8]. This allows the pathogen to reside inside a phagosomal compartment, with a pH of 6.0 - 6.4, avoiding the more acidic and hostile environment of the lysosome, with a pH < 5 [11].

The compartment containing the mycobacterium may be arrested in development but it is by no means static. They are still accessible to fusion with recycling endosomes, giving the pathogen access to nutrients such as iron, provided by transferrin and the transferrin receptor [11]. This access to iron is crucial for the success of the pathogen.

In a controversial study performed by van der Wel et al. 2007, evidence was provided for the phagolysosomal escape of *M.tb* into the cytosol of cultured dendritic cells and macrophages after 48 h of infection [12]. This issue caused some debate, due to the difficulties in interpretation of the results, but recently new results reported by Simeone et al. 2012 support these findings, at least under conditions that lead to necrosis. They show that virulent mycobacteria infecting human macrophages escape the phagosome at a later time during infection and that this escape is induced by virulence factors produced by the bacteria. Mutant bacteria lacking these virulence factors do not escape the phagosomal compartment. In addition, they discovered that this feature was a prelude to the death of the host cell, possibly allowing the bacteria to proliferate in the extracellular core of the granuloma, *in vivo*. [13] However, the question of whether or not host cell death is beneficial for the pathogen is still undecided. It should also be noted that there are studies that do not agree with this interpretation. Jordao et al. 2008 showed that *M.tb* and the related pathogen *Mycobacterium bovis* are restricted to phagosomes in different types of macrophages for several days of infection [14].

The contradictions in results concerning tuberculosis just go to show that due to our lack of knowledge on this topic, a complete understanding of the intracellular behavior of this bacterium has not yet been acquired.

1.2 Antimicrobial agents

Due to the problems associated with *M.tb* infection noted above, such as the increasing cases of drug-resistant strains, new therapeutic strategies or agents for TB need to be uncovered. We can either strive to improve existing systems, such as the treatment regimen offered today, or we can look to something entirely new, such as anti-microbial peptides.

1.2.1 Antimicrobial peptides as novel anti-mycobacterial agents

Our airways are covered with a mucin-rich fluid where we can find antimicrobial peptides and proteins. These, in association with the innate immune system, will work together to eliminate foreign objects, such as bacteria, from the airways and alveoli. [15] Based on this, and our general knowledge of antimicrobial peptides, one can conclude that these peptides have the potential to become a new class of therapeutic agents. Some advantages associated with these

peptides include: an individual peptide shows activity towards many different microorganisms, including drug-resistant strains; a different mechanism is applied in their microbicidal activity; and the development of complete resistance is thought to be very unlikely, as it takes a large number of passages in suboptimal concentrations to achieve low levels of resistance. [16]
Collectively, their most important feature is their cationic nature, brought about by their high abundance of positively charged amino acids. This allows the peptides to associate with the negatively charged surface of bacteria and facilitate permeabilization of their membranes [17-19].

Found in humans and other mammals, there are two main antimicrobial peptide families: defensins and cathelicidins [17]. In addition, I will refer to two other antimicrobial peptides: NK-lysin and *Ciona*-molecule against microbes (Ci-MAM-A24), and discuss their potential as novel peptide antibiotics, which have been and are still being extensively researched.

Defensins

Defensins are a family of antimicrobial peptides that are primarily divided into two subfamilies: α- and β-defensins [15, 17]. Defensins are found in cells and tissues that are a part of the host's defense against pathogens and in many animals they are most often found in granules of either leukocytes [20] or Paneth cells of the intestine. After permeabilization of a bacterial membrane, the biosynthesis of most macromolecules (DNA, RNA, proteins and lipids) is inhibited, no doubt adding to the lethal effects of these peptides [17, 21].
In addition to their killing capacities, some defensins have been reported to have chemotactic abilities towards various immune cells (monocytes, dendritic cells and T cells) [17, 22].

α-Defensins are mainly produced by neutrophils and there are six of them: human neutrophil peptides (HNPs) 1-4 are found in the azurophilic granules of neutrophils [20], while α-defensins 5 and 6 can be found, as mentioned above, in Paneth cells in the intestine [23].
α-Defensins have been found at significant concentrations in the plasma and bronchoalveolar lavage fluid of patients with TB, indicating that they play a crucial role in the host's defense against *M.tb* [24]. This and their known microbicidal effects lead to the natural thought of using them as anti-mycobacterial agents.
Indeed, HNP-1, -2 and -3 have been shown to have microbicidal activity against a wide range of microorganisms [20], including mycobacteria [25]. More specifically, an *in vitro* HNP-1

concentration of 50 µg/ml was reported to kill *M.tb* by Miyakawa et al. in 1996 [26]. One of the follow-up experiments done by Sharma et al. showed that culturing *M.tb*-infected macrophages in the presence of 5 mg/ml HNP-1 was sufficient to kill ~47 % of intracellular bacteria after 3 days of treatment [27]. Later, the same group made an even more convincing case for the potential of HNP-1 as an anti-mycobacterial agent by using it to treat mice infected with TB. After treatment, a significant decrease of CFU (colony forming unit) was accomplished in mice. [28]

β-Defensins are mostly expressed in various epithelial tissues [17] and all human β-defensins (HBD 1-4) are expressed in the airway epithelia [15]. HBD-1 alone has been shown to have anti-mycobacterial activity against *M.tb in vitro*, and even more so in combination with the antibiotic isoniazid [29]. Even so, the most promising work has been done with HBD-2. Human alveolar macrophages do not express defensins naturally, not even upon challenge with *M.tb*; these peptides are expressed by lung epithelial cells [30]. Since these macrophages are most likely the first cells a mycobacterium encounters, one might expect that this is the location were the highest concentration of antimicrobial peptides should be. Therefore, Kisich et al. 2001 took matters into their own hands and used mRNA encoding HBD-2 to transfect into and treat *M.tb*-infected macrophages. They reported a high transfection-efficiency and subsequently also enhanced microbicidal activity leading to inhibition of bacterial growth compared to controls. [31]

Even though different methods are used in these examples, the combined message is clear: defensins have the potential to be used as effective peptide antibiotics against *M.tb*.

Cathelicidin

Cathelicidins are a family of antimicrobial peptides that take part in the innate immunity of mammals. The peptides are characterized by their conserved N-terminal domain, called the cathelin domain, but they also contain a heterogeneous C-terminal domain which, after proteolytic cleavage, will induce the peptide's antimicrobial activity. We only know of one human cathelicidin, LL-37, which is the C-terminal domain of human cationic antimicrobial protein 18 (hCAP18) [32]. Cathelicidin is found throughout the body in different cell types ranging from epithelial cells [33] to different leukocytes (natural killer (NK) cells, macrophages, T cells etc.) [19]. It has broad-spectrum microbicidal activities; it kills both Gram-positive and Gram-negative bacteria [15, 34]. Most importantly, it has shown to be

important during *M.tb* infection. Rivas-Santiago et al. 2008 [35] reported the presence of cathelicidin in *M.tb*-infected lung epithelial cells, neutrophils, monocyte-derived macrophages and alveolar macrophages, in which alveolar macrophages presented the highest levels of expression. In addition, cathelicidin was shown, by electron microscopy, to associate directly with phagocytosed *M.tb* but the peptide was not detected in granulomas, indicating its primary role is during early infection. More directly, Liu et al. 2006 have shown that up-regulation of cathelicidin leads to increased intracellular killing of *M.tb* [36].
Cathelicidin has also been shown to have chemotactic abilities, specifically towards polymorphonuclear leukocytes and $CD4^+$ T cells. This indicates that cathelicidin, like defensins, can function as a bridge between innate and adaptive immunity, and more generally that antimicrobial peptides can have a dual function in TB infection: as a peptide antibiotic and as a signaling molecule that helps to attract key immune cells to the sites of infection.

NK-lysin

NK-lysin is an antimicrobial peptide isolated from pig NK cells and cytotoxic T cells, and is homologous to human granulysin [37, 38]. It is stored in granules produced by these cells and has shown microbicidal activity towards a range of pathogens [37], including mycobacteria [18, 38]. NK-2, a shortened version of NK-lysin, was shown to kill 70 – 80 % of mycobacteria in culture and decrease the bacterial load in infected macrophages, without any cytotoxic effects [18]. Specifically, both synthetic versions and native NK-lysin have been shown to inhibit *M.tb* growth; 90 % inhibition for the synthetic peptides and 60 % inhibition for the native peptide [38].

Ci-MAM-A24

A novel family of antimicrobial peptides was reported by Fedders et al. in 2008 after they had identified them in the sea squirt *Ciona intestinalis* using bioinformatics tools, and with this information they made a synthetic peptide corresponding to its cationic core, namely Ci-MAM-A24. The native peptide was localized to specific granule containing haemocytes and its synthetic counterpart was shown to have microbicidal activity towards a wide range of microorganisms. In addition, it was found to be very salt-tolerant making it suitable for human physiological conditions. [39] In association with mycobacteria, Ci-MAM-A24 was

found to kill 45 – 78 % of bacteria *in vitro* at micromolar concentrations. In cell culture, mycobacterial killing was non-significant and Ci-MAM-A24 appeared to have partial cytotoxic effects on macrophages, in contrast to what had been reported before for erythrocytes. Interestingly, Ci-MAM-A24 in combination with NK-2 facilitated the best killing, both extra- and intracellularly, and together showed no cytotoxicity towards macrophages. [18]
Later it was discovered that Ci-MAM-24 had very potent microbicidal activity towards drug-resistant strains as well, such as methicillin-resistant *Staphylococcus aureus* (MRSA) [40], underscoring the promising potential these peptide antibiotics have as novel therapeutics.

1.2.2 Antibiotics and other anti-mycobacterial agents

Antibiotics – Rifampicin

For treatment of TB we have four first-line antibiotics: isoniazid, rifampicin, pyrazinamide and ethambutol. A treatment regimen usually consists of a combination of these drugs: isoniazid and rifampicin or isoniazid, rifampicin and pyrazinamide. [41] This multi-agent therapy for TB was proposed after streptomycin resistance was observed already in the early clinical trials, shortly after that drug had been introduced [42].

Rifampicin (RIF), discovered in 1965, is a descendent of rifamycin, an agent isolated in 1957 from the bacterial species *Amycolatopsis rifamycinica*. In addition to RIF, there are several antimicrobial agents in the rifamycin family today, all developed through subsequent chemical modifications. [43] RIF has a significant effect on metabolically active *M.tb* and shows late sterilizing action towards semi-dormant organisms, that are induced to undergo sudden bursts of metabolic activity. This late effect of RIF has allowed treatment of TB to be reduced from 1 year to 6 months, highlighting the important role RIF plays in TB therapy. RIF's antibacterial activity is attributed by its ability to bind and inhibit DNA-dependent RNA-polymerase, thereby inhibiting transcription, and as a consequence protein expression. Resistance to RIF occurs via mutations within the gene that encodes the β-subunit of the RNA polymerase. However, resistance to RIF by itself is rare. Usually, resistance towards RIF only occurs in strains that are already resistant to isoniazid, which is how multi-drug resistance is defined in TB patients. [44] The clinical concentration of RIF is very high; 600 mg/day [45]. Consequently, there is some risk of hepatotoxicity with the use of RIF and even higher risks

are associated with the combined use of RIF and isoniazid; but in general, RIF is a well-tolerated drug [46].

Phenothiazines – Thioridazine

Phenothiazines are a group of related compounds that possess many different characteristics; one being anti-tubercular activity. Traditionally, phenothiazines have been used as anti-psychotic agents but their anti-tubercular activity has also been known for quite some time. Due to the discovery of potent antibiotics such as rifampicin, and the adverse side effects associated with these compounds, the phenothiazines were set aside. Now that drug-resistance has become a problem, their potential has again been recognized. [5]

The most potent phenothiazines are thioridazine (TZ) and chlorpromazine, but due to the high level of toxicity associated with chlorpromazine, TZ is usually chosen for use in infection-studies [47]. TZ is thought to have several microbicidal activities: increase in macrophage killing efficiency; reversal of drug resistance; inhibition of gene expression of efflux pumps, but most importantly, it also inhibits bacterial efflux pumps directly. Drug-resistant bacteria are known to have efflux pumps that extrude antibiotics before they get a chance to affect the bacterium in any way. Inhibition of these pumps by TZ makes resistant bacteria susceptible to the drug again. [48]

Initially, it was deemed a problem that *in vitro* concentrations (15 – 30 µg/ml, depending on drug-susceptibility) [49] were far exceeding the limit of what could be used *in vivo* (0.5-1 µg/ml, used in long-term anti-psychotic treatment) [5], but because macrophages concentrate phenothiazines up to 100-fold, one can safely use a low concentration and at the same time achieve intracellular mycobactericidal activity [50, 51]. Indeed, 0.1 µg/ml of TZ was shown to kill both antibiotic-susceptible and MDR strains of *M.tb* within 1 day post infection in macrophages [49]. This 100-fold concentration by macrophages could be the result of TZ affecting macrophage efflux pumps as it does bacterial efflux pumps.
In vivo results with TZ show significant killing of the bacteria in mice infected with drug-susceptible *M.tb*, even more so in combination with first-line antibiotics. TZ activity was also shown to induce significant killing when infection was caused by an MDR-TB strain. [52]

Many questions concerning TZ still need to be answered but the data show that it can be used in defeating an infectious agent such as *M.tb.* In combination with traditional antibiotics, TZ

can help bring these antibiotics back to their Golden-era; when their activities changed TB therapy to the better.

1.3 Zebrafish and *Mycobacterium marinum* as model systems to study tuberculosis

1.3.1 The zebrafish (*Danio rerio*)

The zebrafish was first identified in the river Ganges in India by Francis Hamilton in 1822 [53], but the man who opened the scientific world's eyes to the zebrafish, *Danio rerio*, as a model organism, was George Streisinger, who began working with the fish in the late 1960s. He used the zebrafish to study embryonic development through mutational analysis [54] but before him this fish had already been used to study embryogenesis for more than 100 years [55]. Some of the reasons for why this is such a good model are: the fact that the organism has a short generation time; a single female can produce up to 200 embryos per mating; they are of small size and can be kept at high population density (5 fish/liter); mutagenesis is easily performed; embryos develop externally; and due to their transparency at the embryo- and early larval stage, many processes can readily be visualized through light microscopy. [54, 56] Also, transparent mutants exist that retain their transparency throughout life [57].
In addition, many genetic analyses can be performed on the zebrafish: both forward and reverse genetic analyses; microarrays and mutants are commercially available; and gene-specific, transient knockdown can be performed using morpholino oligonucleotides. Morpholinos are antisense oligonucleotides that block RNA translation, either by binding to the translational start site or intron-exon junctions to create non-functional splice variants [58].

Zebrafish embryos have also proven to be useful for chemical screens, because of their small size and the fact that they can absorb chemicals that are present in their aqueous environment through their skin. The compound of interest can, therefore, easily be administered to the water and the effects can readily be observed [56, 59]. This again gives us the advantage of studying the effects of novel anti-microbial agents *in vivo*.

When it comes to immunological studies the zebrafish has one big advantage. As an adult the zebrafish has both adaptive and innate immune responses, but at the embryo and larval stages,

only the innate immune system is functional. T cell progenitors migrate to the thymus at 3 days post fertilization (dpf) but the adaptive immune system does not become functional until 4 – 6 weeks post fertilization [60]. This makes it possible to study the factors of innate immunity without interference from the adaptive immune system. In a paper published by the Ramakrishnan group, they use this to their advantage when they disprove the preconceived notion that adaptive immunity is crucial for granuloma formation in tuberculosis, with the use of zebrafish embryos and *Mycobacterium marinum* (*M.marinum*) [61].

1.3.2 *Mycobacterium marinum*

Like *M.tb, M.marinum* is a rod-shaped bacterium, with unique lipids called, mycolic acids, present on its surface. This makes the surface waxy and hydrophobic, and prevents the use of the traditional Gram stain. Instead an acid-fast Ziehl-Neelsen stain needs to be used [62]. It is an aerobic bacterium that grows optimally in the dark. When grown in the light, pigments are produced, consistent with it being defined as a photochromogen [63]. This bacterium is an aquatic organism, naturally infecting fish and amphibians. Therefore, its optimal growth temperature naturally lies between 25° and 35°C. *M.marinum* has a generation time of 6 – 8 hours [63], making it a fast grower compared to *M.tb*, which has a generation time of more than 20 hours. Because it does not grow well in the human body at a temperature of 37°C, if infected, one tends to find infectious lesions in the cooler, superficial regions of the human body, which are referred to as swimming pool granulomas. *M.marinum* very rarely causes a systemic infection. [64]

Tønjum et al. 1998 suggested that *M.marinum* could be used as a model organism for *M.tb*. They performed gas chromatography of fatty acids and alcohols, DNA-DNA hybridization, and 16S rRNA gene sequence analyses to clarify the relationship between four different mycobacterial species; *M.marinum* being one of them. What they found was two mycobacteria, *M.marinum* and *Mycobacterium ulcerans*, that were more closely related to *M.tb* than any other mycobacterial species (Figure 3) [65].

In addition to being close relatives, *M.marinum* and *M.tb* appear to "behave" the same way. They are both phagocytosed by macrophages, inhibit the maturation of the phagosome into a phagolysosome, and they produce granulomas with the same characteristics in their natural hosts [64, 66].

Through the pioneering work of Lalita Ramakrishnan and her group, it has unequivocally been demonstrated that *M.marinum* is a good model for studying *M.tb* in humans. [56, 67, 68]

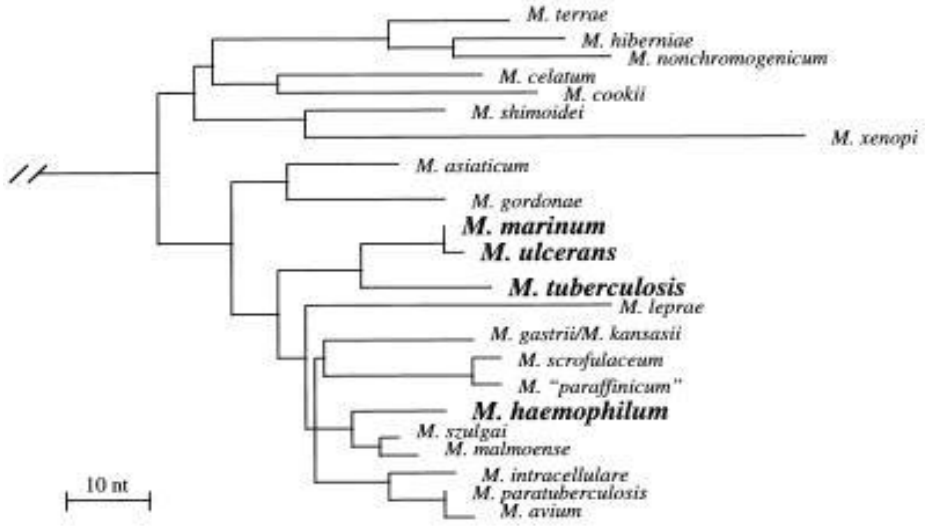

Figure 3: Phylogenetic tree showing the genetic relationships between mycobacterial species. The figure is taken from Tønjum et al. 1998 [65].

1.3.3 The zebrafish as a model for studying infectious disease

The relationship between host and pathogen is a complex one. So when developing novel drugs against infectious diseases, or in our case a drug delivery system, an animal model is needed. Drugs that show promise *in vitro* may not have the same effect *in vivo* [56].
It has been shown in several reviews that the human and zebrafish immune systems are surprisingly alike, for example homologues of all 10 human Toll-like receptor (TLR) families have been identified in zebrafish [69-71]. In addition, expression of NK-lysin in zebrafish has been proven [72] and 3 β-defensin like genes have been identified [73], meaning, as in humans, antimicrobial peptides are important components of the innate immune system.

The advantages listed earlier (transparency, *in vivo* imaging, mutagenesis, etc.) are characteristics that make the zebrafish a strong vertebrate model for studying infectious diseases.

The *M.marinum*-zebrafish model for human tuberculosis

There are several model organisms used for the study of tuberculosis and even though humans are its natural host, all of them are susceptible to *M.tb* infection. The mouse has mostly been used for these studies. This is due to the vast amount of knowledge and molecular tools, such as antibodies, we already have for this organism, but there are also some disadvantages: latent infection is hard to obtain and the granulomas that form are quite different from human granulomas. Usually human granulomas are well-defined and organized structures that often develop a caseating necrotic core. In mice the granulomas that form during infection are the opposite: they are not organized and they do not develop a caseating necrotic core.
Other models include guinea pigs, rabbits, and non-human primates, all with their own advantages and disadvantages. Guinea pigs for example form human-like granulomas but are extremely sensitive to the disease and die rapidly [74].

In addition, we now also have non-mammalian model organisms, namely the leopard frog (*Rana pipiens*) and the zebrafish, which can be infected with *M.marinum*. The leopard frog has been shown to develop non-caseating and tightly organized granulomas and the infection produced is long-term with no symptoms, making this a good model for latent TB infection [75, 76]. When it comes to adult zebrafish, infection with *M.marinum* causes the production of organized and caseating granulomas, which are very similar to human granulomas, an important factor that shows how suitable the *M.marinum*-zebrafish model is to study active tuberculosis [66, 75]. This has also been shown to be the case upon infection of embryos [61].

Also, the *M.marinum* and *M.tb* infections themselves have proven to have many similarities. In addition to zebrafish-specific TLRs, infection with *M.marinum* has been shown to induce expression of TLRs that are homologues of human TLRs expressed during human TB infection [71].

The zebrafish embryo model makes *in vivo* imaging of interactions between the host and the pathogen possible, and mutational analysis of both host and pathogen can be performed, as done in the Ramakrishnan group. One of the first major observations made in this system helps to rationalize how *M.tb* can survive essentially for dozens of years as an intracellular pathogen, when macrophages normally have a life-span of a couple of weeks [77]. Davis et al. 2002 saw that uninfected macrophages can be induced to migrate towards the infected macrophages in granulomas, which was later shown to be mediated by the bacterial secretion

of specific virulence factors, which will be discussed in more detail below [61, 78]. They also witnessed, for the first time, an uninfected macrophage phagocytosing another macrophage infected with *M.marinum*, which has been shown to be a means of bacterial dissemination; allowing passage of the infection from one macrophage to another without interference from the immune system [61].

Further innovative use of this system went into comparing the pathogenesis of wild-type (WT) *M.marinum* to a mutant they call ΔRD1. This mutant is lacking the RD1 (region of difference 1) locus, the same locus that is missing in attenuated bacille Calmette-Guérin (BCG) vaccine strains [78]. The locus encodes a secretion system for mycobacterial virulence factors, also encoded within the same locus, that are injected via the secretion system into the host cell. Of these factors, the best characterized are ESAT-6 (6 kDa early secretory antigenic target) and CFP-10 (10 kDa culture filtrate protein), which are vital for the virulence of mycobacteria; namely, granuloma formation and bacterial dissemination therein [78, 79]. With these results, and those from Cosma et al. 2004, where superinfecting *M.marinum* were shown to penetrate pre-existing granulomas and thrive there [80], the traditional view of the granuloma as a purely host-protective structure was greatly challenged.

In another powerful example of the strength of this model system, the same group used a morpholino to knock out the myeloid transcription factor gene *pu.1*, which is needed for the differentiation of macrophages; thereby creating embryos without macrophages. With this approach, they discovered that when the *pu.1* mutant zebrafish were infected with WT *M.marinum*, the bacterial burden was 10-fold higher than in the control fish with macrophages at 4 days post infection (dpi), suggesting that early on, macrophages play a crucial role in controlling the infection. This result was in support of the granuloma being a host-protective structure, where macrophages greatly reduce bacterial growth.
On the other hand, upon further inspection they also established that the mycobacteria are fully dependent on macrophages to cross the epithelial barriers. [81] Taken together these results show the "give and take" relationship that has evolved over time between host and pathogen and the dual role the macrophage plays during infection; limiting bacterial numbers and enabling the bacteria to disseminate into deeper tissues where they can establish an infection [81].

These are just some examples of the high quality of work that has come from the Ramakrishnan group over the past years, which are summarized in a review by Ramakrishnan

in 2012 [82], where their collective results shine a new light on the traditional view of the granuloma. The granuloma no longer "walls off" the infection and creates a barrier in which almost no bacterial proliferation occurs. It is a dynamic, and also a pathogen-favorable structure. Mycobacteria are able to exploit granuloma formation for their proliferation and dissemination, both within the granuloma and to other sites in the body where a new granuloma can be initiated. Instead of blocking immune responses the bacteria seem to accelerate them to use to their advantage, such as the constant recruitment of macrophages to the granuloma, which facilitates bacterial dissemination [82, 83].

Overall, the large body of work carried out by the Ramakrishnan group, as well as others, make a compelling case that the *M.marinum*- zebrafish model is a powerful system that gives important insights that are relevant for understanding the pathogenesis of *M.tb* [56, 67, 68]. All these reasons are in support of our choice to make use of this model system.

1.4 Nanoparticles in therapy of infectious disease

1.4.1 Background

Antibiotics are traditionally administrated orally in the form of tablets and the oral absorption of, for example RIF, is controversial. During the first hours after administration, plasma levels peak and eventually the drug is broken down by the liver or excreted through the kidneys. [45] This systemic release may lead to toxic side-effects [46] and depending on the physicochemical properties of the drug, may not reach its target site in a therapeutic concentration [84]. The advent of nanotechnology has provided a more attractive concept for drug delivery, in the form of biodegradable polymer nanoparticles (NPs) that can be formulated such that the drug is enclosed (and protected) in the NP. As the NP-containing endo-/phago-somal compartment matures the pH will decrease and degradation of the NPs will lead to subsequent drug release [85].

In our case the encapsulation of drug means the drug is entrapped in the polymer matrix of the particle, which is then called a nanosphere. Throughout this thesis this type of particle will simply be referred to as a nanoparticle (Figure 4).

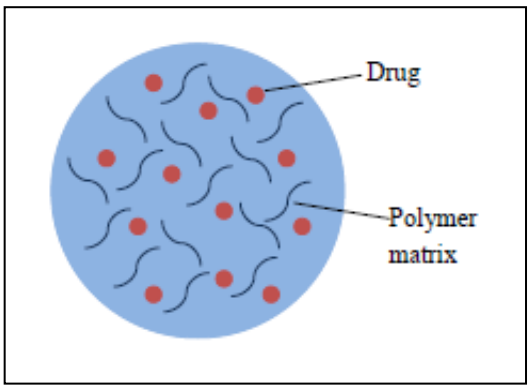

Figure 4: Illustration of a nanosphere. The drug is dispersed throughout the polymer matrix.

After learning of the work of Gopal Khuller and his group (which will be decribed in more detail later), where encapsulated anti-tubercular drugs were being used in animal models to treat tuberculosis, we decided to combine his work and the work of Lalita Ramakrishnan (mentioned earlier), to work towards a better understanding of TB pathogenesis and more importantly, treatment.

1.4.2 Nanoparticle formulation

NPs are defined as being less than 1 µm in diameter and are made of natural or synthetic polymers [86]. Some examples include poly (lactic-co-glycolic acid) (PLGA), poly-lactic acid, chitosan, alginate, and lipids, to name a few [87]. The most widely used is PLGA, a polymer that has long been approved for use in humans by the US Food and Drug Administration. It is biocompatible and biodegradable, two crucial characteristics for NPs in drug therapy [85].

NPs can be used for the encapsulation of many different agents: hydrophobic drugs, hydrophilic drugs, proteins and peptides, vaccines, and biological macromolecules, such as plasmid DNA (pDNA) [86]. Our group's starting point was the encapsulation of the hydrophobic antibiotic RIF, this being based on the success of Gopal Khuller and others in this area, which will be mentioned later.

There are several preparation methods for NPs. Which method one chooses depends mainly on what needs to be encapsulated. For hydophobic compounds, such as RIF, the most common NP preparation technique can be used: the emulsion-solvent evaporation technique, also called a single emulsion or oil-in-water (o/w) emulsion. For hydrophilic compounds, such as DNA, and proteins you can use a modification of this technique, a so-called double

emulsion or water-in-oil-in-water (w/o/w) emulsion [86]. Another method that can be used for encapsulation of both hydrophilic and hydrophobic compounds, is nanoprecipitation, where no emulsion is prepared because the particles form spontaneously [88, 89]. This method will be explained later in more detail for the encapsulation of pDNA.

Modifications to the NPs can be made. We know that specific cell surface receptors can either be over-expressed or expressed exclusively in specific tissues, and this can be used to our advantage by binding the corresponding ligand to the surface of NPs. With this and monoclonal antibodies available one can facilitate targeted and sustained treatment. [84, 90] One example of such is mannose. Mannose receptors are found on the cell surfaces of macrophages and dendritic cells and the presence of mannose on the surface of NPs may promote a higher uptake by macrophages, compared to unmodified NPs [91]. In another example, coating of NPs with the lectin, wheat germ agglutinin (which binds sialic acid and N-acetylglucosamine), will facilitate the binding of NPs to intestinal and alveolar epithelium, making them suitable for both oral and aerosol delivery. Because of this "entrapment" at a specific site in the body, the presence of drug in plasma has been shown to be prolonged in comparison to NPs without lectins, making it possible to decrease the dosage number [92].

1.4.3 Nanoparticles and tuberculosis

As in the case of TB and other intracellular pathogens, treatment usually involves long-term therapy with a combination of drugs. Due to the length of therapy, and the often frequent administration of drugs, side-effects due to toxicity commonly arise, leading to patient non-compliance that again can lead to the development of drug-resistant bacteria. In addition, the cost of this treatment regimen is high. [6, 87]
In general, to treat intracellular pathogens, a sufficient amount of active drug needs to reach the compartment in which the pathogen is hiding, whether it be the phagosome (as in the case of TB), a vacuole (Salmonella) or the cytosol (Listeria) [8, 93, 94]. To get to these compartments a drug needs to cross the cell membrane, reach the pathogen, and do so in a high enough concentration as to reach therapeutic levels, which may be a problem depending on the molecule's physicochemical properties [84, 87]. In addition, many drugs are unfortunately very toxic, not only do they kill the pathogen, they also damage healthy tissue [84]. These are the obstacles nanotechnology can help us bypass.

Upon administration, whether it is through injection, oral, or aerosol, the NPs are identified by the immune system as foreign objects. Phagocytic cells, such as macrophages, will naturally engulf the NPs. In terms of using NPs as therapy against TB, this is very advantageous. As described above, *M.tb* is an intracellular pathogen of macrophages, the same cells that later will make up most of the granuloma. In this case, designing a targeting system is not essential as the NPs are naturally targeted to the infected cells and eventually the site of infection itself, the granuloma, where they can facilitate targeted and sustained release of the drug. [9, 84, 87] Actually, upon uptake of microparticles containing antibiotics, the intracellular drug concentration in macrophages compared to the extracellular concentration when free drug is used, has been shown to be up to 10 times more [95]. This indicates how advantageous NP-based drug delivery can be in treatment of intracellular pathogens.

As mentioned, TB therapy is tedious and costly and often leads to non-compliance in patients. Creating a drug delivery system that can overcome these obstacles and provide a sustained and site-specific drug release would be most advantageous. With this we can avoid the toxicity issues when taking drugs for a long period of time by lowering the dosage amount and the frequency of drug administration [87, 96].
Through the work of Gopal Khuller and his group we have learned just how effective treatment with NPs can be. They have shown that by both oral [97, 98] and aerosol [99] administration of anti-tubercular drug-loaded NPs, sustained drug delivery is accomplished. The oral administration of free RIF versus encapsulated RIF is depicted in Figure 5. Here we can see that free RIF peaks early and clears the body in 24 h. The RIF-NPs on the other hand facilitate a so-called “burst release”, thought to be facilitated by drug in association with the NP surface [86], and then sustained release is established in plasma for 6 days. In the tissues however, therapeutic levels of drugs could be detected for 10-11 days. This allowed *M.tb*-infected animals to receive therapy every 10 days instead of the traditional daily dose of free drug during a 46 day monitoring period. Meaning, 5 doses of RIF-NPs can replace 46 daily doses of free drug and still clear the infection [97, 99]. In addition this therapy was further improved by coating the PLGA NPs with a lectin. As explained above, the drug remained at therapeutic concentrations in the plasma for a longer period of time as compared to drug released from unmodified NPs, making it possible to decrease the number of NP doses from five (as noted above) to three. [92]

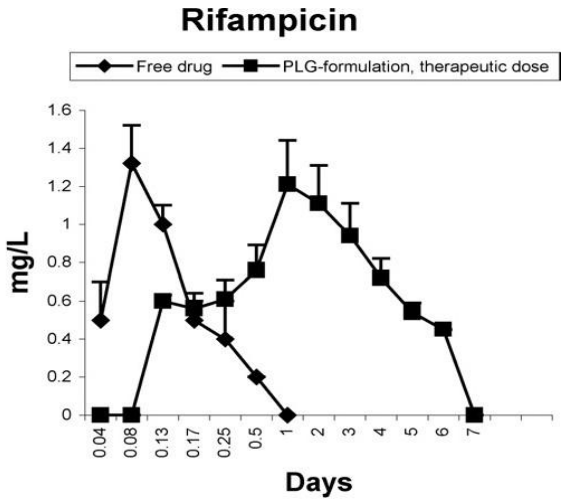

Figure 5: RIF concentration after one oral administration of either free or encapsulated drug to mice. Taken from Pandey et al. 2006 [96].

The advantages are clear: (1) frequency of dosage is greatly reduced so non-compliance should not be as big a problem (it is also foreseen that this property would be an advantage in treating drug-resistant strains); (2) the local concentration of drugs (intracellular) is higher than the systemic concentration, leading to reduced toxicity [95]; (3) targeted and sustained release of the drug is accomplished at therapeutic concentrations; and (4) the amount of drug needed for therapy can be reduced, making the therapy less costly. This was shown by Sharma et al. 2004 with the use of NPs loaded with two-thirds of the therapeutic dose to clear an *M.tb*-infection in guinea pigs. This was done over the same time-period as mentioned above (46 days) with the same number of doses (5 doses) [98].

1.4.4 Nanoparticles and DNA

Another promising field of NP-based delivery systems is DNA delivery, whether it is as vaccines or gene therapy the advantages are many. We were interested in this approach because of the attractive possibility of encapsulating pDNA encoding anti-microbial peptides, e.g. LL-37, that have been shown to be effective against *M.tb* and other mycobacteria both *in vitro* and *in vivo*.

In the case of oral administration of drugs, there are critical obstacles to overcome: the hostile environment of the stomach and crossing the epithelial layer in the intestine to reach circulation. In addition to the obstacles mentioned earlier, for DNA delivery there are additional obstacles: the need to cross the endosomal membrane and after entering the cytoplasm, to enter the nucleus [100]. NPs can help to overcome these obstacles.

An ideal DNA delivery system should fulfill some requirements: (1) the particles should contain a high amount of intact DNA; (2) the polymer should protect the DNA against nuclease degradation; and (3) the burst release should be as low as possible to avoid loss of DNA. [101]
These requirements have proven difficult to achieve but advances have been made.
DNA carrier systems made of PLGA are mostly produced using the double emulsion-solvent evaporation technique, but there are usually some problems associated with this procedure. During production, DNA comes into contact with organic solvents and is subjected to the shearing effects of sonication or homogenization, possibly leading to the destruction of the molecule. [102, 103] Many solutions have been provided to circumvent these problems, the most drastic being the use of a different polymer, such as chitosan, a natural polymer that is considered non-toxic and biodegradable, has mucoadhesive properties and can increase cellular permeability [100].
Opinions, and results, differ on how much damage DNA suffers under the conditions of particle preparation. Some show that the polymer itself protects DNA from both shearing and nuclease activity [104, 105], while others propose the use of protective buffers during the process [106]. Others again suggest the use cationic polymers, such as polyethyleneimine (PEI) [107] and polyethylene glycol (PEG) [103], to form complexes with DNA before the encapsulation process. This provides some protection, and in the case of PEG, it also allows for dissolution in organic solvents such as dimethyl sulfoxide (DMSO) [108].

To avoid the shearing of the emulsion-solvent evaporation technique all together, there has been one report of the successful encapsulation of pDNA in PLGA NPs with the use of the nanoprecipitation method [109]. This method does not require the use of sonication or homogenization to create particles, they develop spontaneously, but the method does require the use of an organic solvent [110].

Like other endo-/phago-cytosed NPs after internalization, DNA-NPs will travel through the endo-/phago-lysosomal pathway where they are subsequently degraded. A prerequisite for treatment will be the escape of intact DNA to the cytosol, where it can translocate to the nucleus for transcription [111]. NP/pDNA escape from the endo-/phago-somal compartment is a highly debated topic but most agree it is necessary for the DNA, in some way, to escape the detrimental environment of the endo/phago-lysosome [84, 111]. In a highly cited paper by Panyam et al. 2002, they claim endo-lysosomal escape of unmodified PLGA NPs through

what they call a “selective reversal of the surface charge of NPs (from anionic to cationic)”. When cationic, the NP will interact with and destabilize the membrane of the endo-lysosome and escape to the cytosol [112]. The results of our group do not agree with this interpretation of Panyam and colleagues; in our results the NPs with RIF and the fluorescent dye coumarin-6 remain in phagolysosomes where the polymer is degraded (Kalluru et al., in prep.). However, the fact remains that in the case of DNA-NPs some of the free DNA must be able to cross the membrane of the endocytic compartment and enter the nucleus in order to be expressed. Specific chemicals are often included in the NP formulation to facilitate this process. Usually this compound has a buffering capacity at the acidic pH of the endo-/phago-lysosomal compartment. An example of such is PEI, which works as a “proton sponge”, causing osmotic swelling and subsequent disruption of the membrane [113, 114].

Ongoing work will surely shed some more light on this issue in the future.

2 Aims of study

This Master's thesis can be separated into two parts: (1) experiments related to improvement of TB drug therapy using the *M.marinum*-zebrafish embryo model system, and (2) encapsulation of plasmid DNA encoding an antimicrobial peptide.

In TB drug therapy my aims were to:

- Predict the treatment outcome in using RIF-NPs in the *M.marinum*-zebrafish embryo model system, namely identify which concentrations cause toxicity and can eradicate the bacterial infection.

- Evaluate the anti-mycobacterial effect of thioridazine, alone and in combination with traditional antibiotics, in the *M.marinum*-zebrafish embryo model system.

For pDNA-encapsulation my aims were to:

- Establish a protocol for encapsulation of plasmid DNA by use of the nanoprecipitation method.

- Characterize the NPs produced and thereby establish protocols for this purpose.

- Establish pDNA-NP therapy in mycobacterium-infected macrophages and subsequently, zebrafish embryos.

3 Materials and methods

3.1 Zebrafish maintenance and care

Approximately 100 Nacre -/- strain embryos were received from Darren Gilmour (EMBL, Heidelberg, Germany) and grown till adulthood in Peter Aleström's zebrafish facility at the Norwegian School of Veterinary Science. The adult fish were then brought to the Department of Molecular Biosciences (University in Oslo) and put in an Aquatic Habitats Benchtop Aquaria Rack System (Aquatic Habitats, Apopka, FL, USA) to start our fish facility. This system keeps the water well aerated and at a constant temperature of 28°C. Each day, approximately 10 % of the tank-water is exchanged for fresh system water and the light/dark cycle in the room is 12:12 hours. The fish are fed three times a day; once with SDS 400 dry food (Lillicobiotech, Horley, UK) and twice with brine shrimp.

Figure 6: Adult zebrafish of the nacre strain. Its transparent skin allows us to readily identify this fish as female. Image taken from http://www.carolina.com/product/155590.do

The zebrafish can be bred every two weeks. The day before breeding, breeding tanks need to be set up: the bottom of the tanks are covered with a single layer of marbles; the tanks are filled with fresh system water and placed in a water bath to keep a constant temperature of 28°C; and males and females (3 and 2, respectively) are placed in the tanks separated by a splitter and kept overnight. Zebrafish males are slender and have a torpedo-shaped body and they tend to chase females early in the morning before they breed. Females are more easily distinguished, as they are typically fat with eggs, which can easily be observed due to their transparent skin (Figure 6). Zebrafish are photoperiodic and breed at dawn. So, in the morning, before the light cycle begins, the splitters in the breeding tanks are removed and

spawning takes place for approximately two hours. After spawning, the fish are returned to their tanks in the rack and the embryos are collected. Up to 200 eggs can be produced per pair of fish. Collected embryos are kept in embryo water[1] in an incubator at 28°C and the embryo water is changed every day. The embryos will naturally escape the chorion themselves; however, this is undesirable as the chorion material is a haven for bacteria. Therefore, the embryos are manually dechorionated approximately 30 hours post fertilization with fine jeweler's forceps (Dumont No.5).

For fish experiments we either breed nacre zebrafish ourselves (as described above) or wild-type embryos are bought from Peter Aleström's zebrafish facility at the Norwegian School of Veterinary Science in Oslo.

3.2 Culturing *M.marinum*

The following protocols were adapted from the work of Cosma et al. 2006 [115] and Gao et al. 2005 [63].

Our group now has several genetically manipulated strains of *M.marinum*, but mainly either red or green fluorescent bacteria are used for infection studies. For my experiments, only red fluorescent bacteria have been used. The bacteria were generously supplied by Monica Hagedorn at EMBL in Heidelberg, Germany, and they are the human isolate strain ATCC #BAA-535, also called M strain, which carry a construct containing the fluorescent protein DsRed and a kanamycin resistance cassette.

M.marinum grows optimally in vitro at temperatures between 30 to 32°C, has a generation time of 6 to 8 hours in the mid-log phase of growth, and has a biosafety requirement of BSL-2. *M.marinum* is aerobic and it is a photochromogen, meaning its physiology and biochemistry varies in light versus dark; and *M.marinum* grows optimally in the dark. *M.marinum* can be cultured on both solid and in liquid medium, as I will describe. And I will also describe methods for long-term storage.

For culturing in liquid medium, 20 ml 7H9 medium (BD, Franklin Lakes, NJ, USA) supplemented with 40 μg/ml kanamycin (Sigma-Aldrich, St. Louis, MO, USA) and ADC (from here on called 7H9-kan) is aliquoted into a sterile 100 ml glass screw-top reagent bottle

[1] See Appendix for recipe

and warmed up to approximately 31°C. A vial of frozen *M.marinum*-DsRed is thawed on ice for 15 – 20 min and the amount needed is inoculated into the pre-warmed medium. The inoculation amount depends mainly on how quickly one needs the bacteria to reach the appropriate optical density at 600 nm (OD_{600}). According to a growth curve of *M.marinum* that I made (Figure 7), inoculating 1 µl frozen bacteria gives bacteria in the mid-log phase of growth (OD_{600} of ~1.0 – 1.2) in 5 days.

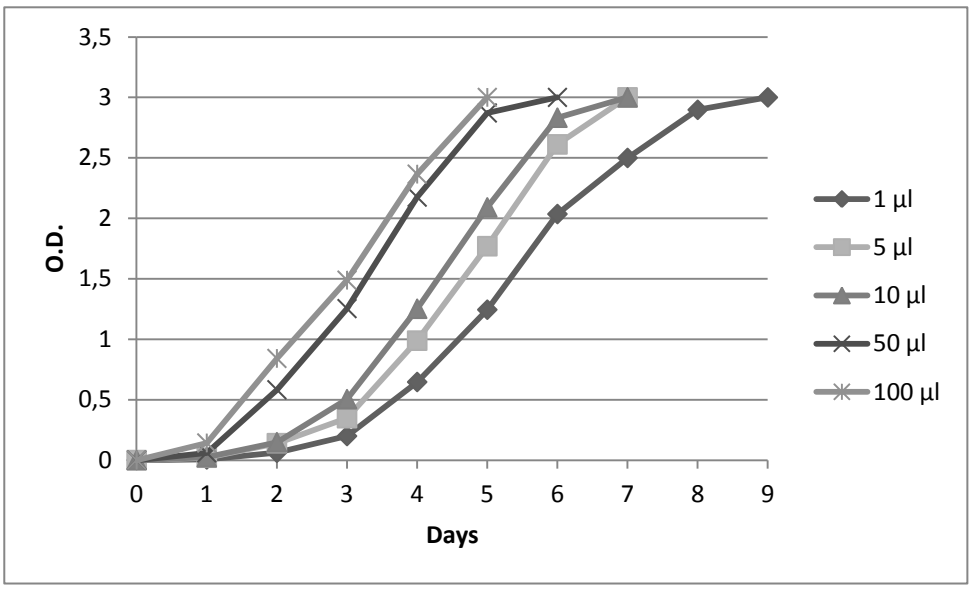

Figure 7: Growth curve of M.marinum-DsRed taken from frozen stock.

If the bacteria are needed faster, a higher inoculation volume can be used. The disadvantages of this are: (1) the culture will contain a higher percentage of bacteria originating from the frozen stock, some of which may not be viable; and (2) the frozen stock will be used up more quickly.

Since *M.marinum* mostly grows in clumps or aggregates, it is important to de-clump the bacteria properly, which can be done in several ways; here we use a syringe fitted with a needle small enough to break up the clumps (22 G needle, BD). The OD_{600} needs to be measured directly after addition to the spectrophotometer cuvette to avoid the effects of possible sedimentation.

After inoculation the lid of the bottle is tightened and the bottle placed in a shaking incubator at 31°C and 100 rpm, in the dark. (The micro-oxygenation under the shaking conditions is sufficient for proper growth)

For culturing on solid medium, transfer 100 µl bacterial suspension to a 7H10 (BD) agar plate supplemented with 40 µg/ml kanamycin and ADC (from here on called 7H10-kan), that has been pre-warmed in a 31°C incubator. Use a disposable spreader to spread the bacteria evenly across the agar surface. One can also dip an inoculating loop in the suspension and spread it on the agar plate. The plates are placed bottom-side-up in an incubator set at 31°C, and left for 5 to 7 days until colonies appear.

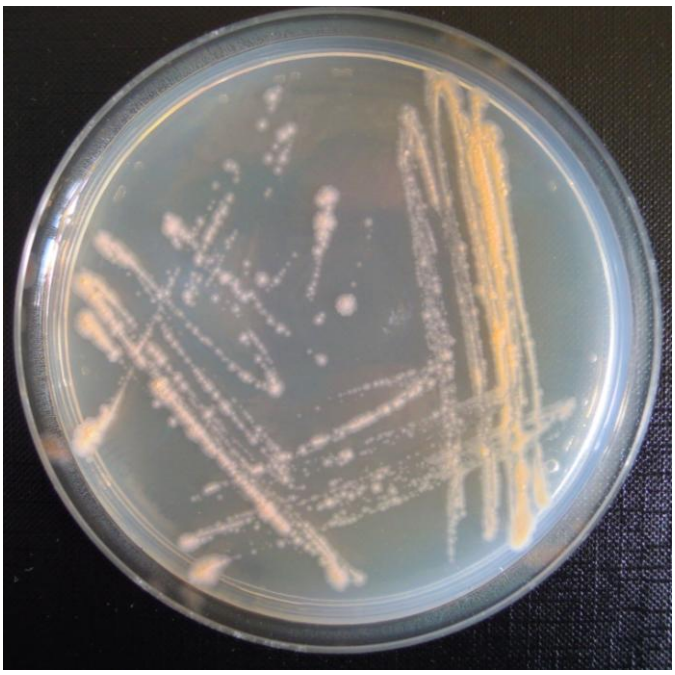

Figure 8: *M.marinum* cultured on solid medium (7H10-kan agar). Colonies have a rough morphology, are irregularly shaped at the edge and waxy as a whole. These colonies are colored red due to the expression of DsRed.

If needed, both liquid and solid cultures can be stored short-term. Liquid cultures can be stored at room temperature, in the dark, for 2 months. The same applies for solid cultures; the agar plates can be sealed and stored at room temperature, in the dark, for 2 months.

For long-term storage one can prepare a frozen stock: 10 ml of the confluent culture (mid- to late- log phase) is transferred to a conical tube and centrifuged for 10 min at 2700 x g at room temperature. The supernatant is discarded and the pellet re-suspended in 10 ml freezing medium[2]. The solution is divided into 1-ml aliquots in cryo-vials and stored at -80°C. Under these conditions *M.marinum* remains viable for over 20 years.

[2] See Appendix for recipe

3.3 Infection of zebrafish embryos with *M.marinum*

This infection protocol was largely established by David Westmoreland for his Master's thesis. Else wise, this protocol was adapted from the work of Cosma et al. 2006 [115].

There are two main locations for injection to choose from: the Duct of Cuvier (1) and the caudal vein (2) (Figure 9). Both injection sites are in the blood flow and the crucial differences are the time at which these injections can be performed and the level of difficulty. The caudal vein injection is the more difficult of the two but it has the advantage that it can be performed at 30 hours post fertilization (hpf), and will therefore give you more time for your experiments, while the Duct of Cuvier is available for injection after 48-56 hpf, the time it takes for the yolk sac circulation to form. Injection fluid is always injected the same direction as the blood flow.

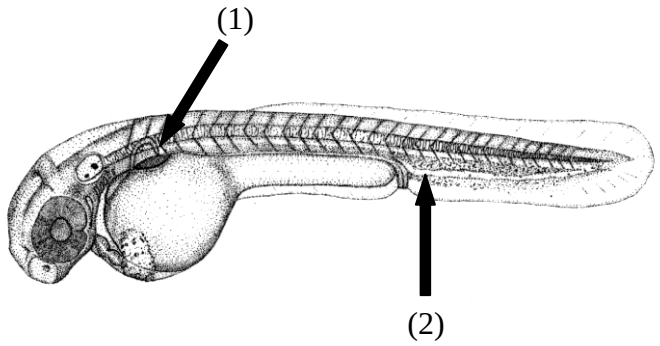

Figure 9: Schematic of zebrafish larvae with arrows indicating the two main injection sites: (1) Duct of Cuvier and (2) caudal vein. Image is taken from http://www.neuro.uoregon.edu/k12/Part%202.html

When the bacterial culture has reached the appropriate OD_{600} for infection (0.8 – 1.5), it is beneficial to check the fluorescence of the bacteria in a fluorescence microscope. This tells you something about the health of your culture. At the same time it is also advisable to check for contamination!

Capillaries of borosilicate (without filament, outer and inner diameter of 1.00 and 0.78 mm, respectively, length of 100 mm, Harvard Apparatus, Holliston, MA, USA) were used to make needles by using a needle puller (P-97 Flaming/Brown micropipette puller, Sutter Instrument, Novato, CA, USA) at the following settings: pressure – 500, heat – 610, pull – 40, velocity – 50, and delay – 110.

Typically 1 ml bacterial culture is taken out and spun down at 17,000 x g for 2 min. The supernatant is removed and the pellet is re-suspended in 1 ml pre-warmed 2 % polyvinylpyrrolidone, PVP (Merck Millipore, Billerica, MA, USA) (the PVP prevents the bacteria from aggregating during injection). This washing step is repeated. If the initial OD is appropriate for injection, one can re-suspend the pellet in 1 ml 2 % PVP. The final OD is measured against a 2 % PVP blank to make sure the OD is still above 0.8. If too many bacteria have been lost during the process, one can take a larger aliquot of liquid culture or reduce the amount of PVP to re-suspend in. When a satisfactory OD has been achieved, the bacterial solution is passed through a 27 G needle (BD) to de-clump the bacteria before injection. 20 % Phenol red (Sigma-Aldrich) is added to the suspension to create a 1 % solution (1 µl phenol red per 20 µl bacterial suspension), this to help visualize the injection. The borosilicate needle is loaded with 5 µl of the bacterial suspension containing phenol red, using a needle-loading pipette tip (Eppendorf, Hamburg, Germany). The needle is attached to the micromanipulator (Narishige, Tokyo, Japan) and pressure controller (FemtoJet, Eppendorf), and the nitrogen gas and pressure controller is then switched on.
A petri dish lid is filled with mineral oil (Sigma) and the injection volume is adjusted to approximately 1 nl, as described by Rosen et al. 2009 [116].

Before infections, one injection is performed in a drop of PBS on a 7H10-kan agar plate to estimate the CFU of the injection volume. This procedure should be performed at intervals throughout the experiment to determine the average amount of bacteria which are injected. When ready for infection, 2-day old embryos are taken from the 28°C incubator and transferred to a tricaine (Argent Laboratories, Redmond, WA, USA) bath (252 µg/ml, pH ~7) to be anaesthetized. After 1-2 min the embryos are transferred to a 2 % agarose (Invitrogen, Life Technologies, Paisley, UK) injection plate and the excess water is removed in order to immobilize them while injecting. The micromanipulator is then used to move the needle to the desired injection site and the injection is performed. The presence of phenol red in the blood stream will be an indicator of a successful injection (Figure 10).

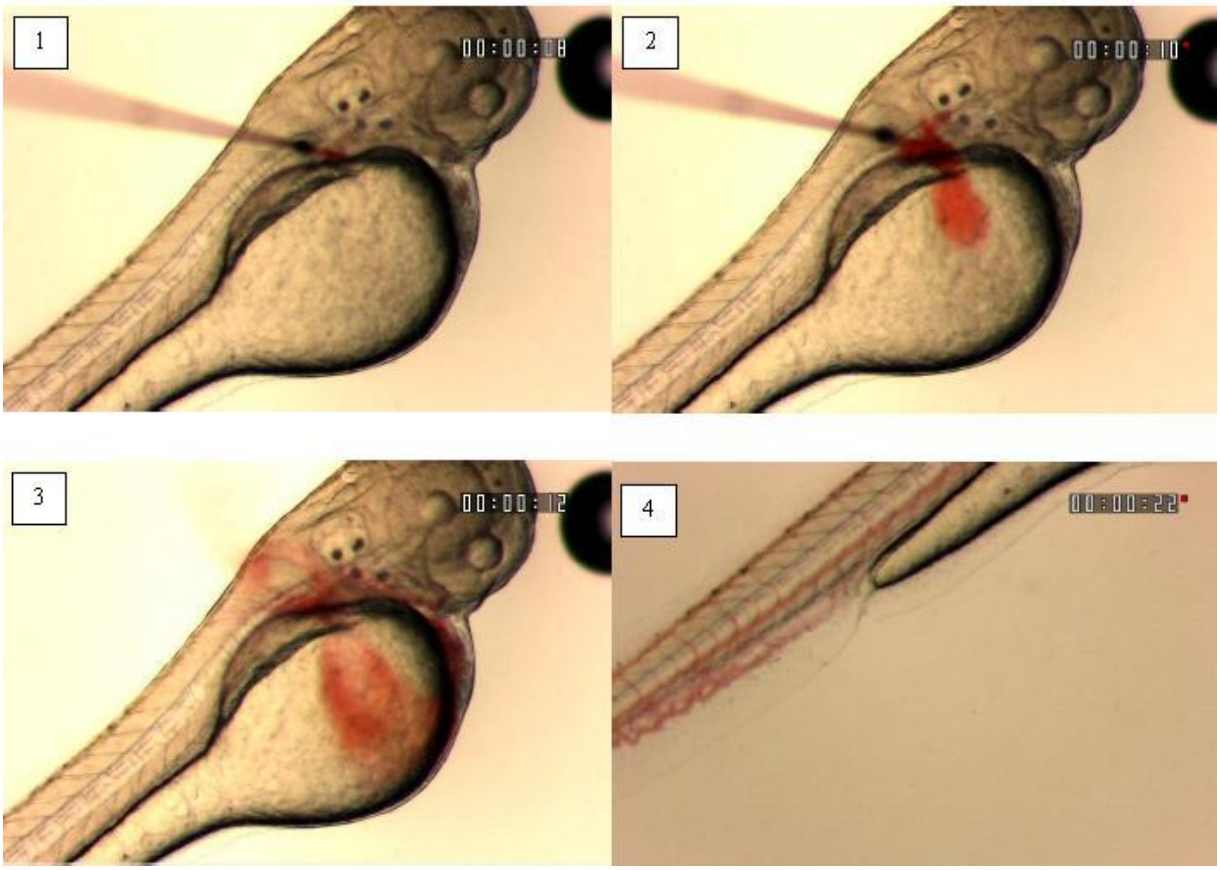

Figure 10: By using phenol red one can clearly separate the successful injections from the unsuccessful. Figure courtesy of David Westmoreland.

Using a pipette, the injected embryos are then transferred into a new dish containing fresh embryo water and eventually placed in the incubator.

The embryos could then be used for monitoring survival or could be picked out at predetermined time-points for gene expression analysis by quantitative PCR. When the latter was the case, the embryos were euthanized in tricaine, placed in the appropriate amount of RNAlater[3] (as recommended by the manufacturer, Ambion, Life Technologies, Paisley, UK), and stored at 4°C until they were ready for use. In this case embryos were collected at 2, 5, 8 and 24 h, and 3 days pi for examination of gene expression.

Gene expression analyses were performed by Henning Fedders in Matthias Leippe's Group at the Christian Albrechts University in Kiel, Germany, as a part of our collaboration with them. The genes of interest were the genes encoding NK-lysins 1-4 in the zebrafish. Comparisons were made between infected embryos and control embryos injected with PBS.

[3] RNAlater is a reagent that stabilizes and protects RNA in tissue samples.

3.4 Infection of adult zebrafish with *M.marinum*

This procedure is largely based on the protocols supplied by Cosma et al. 2006 [115] and Arturas Kavaliauskis, 2011 [117].

Bacteria were prepared as stated above.
The acquired amount of fish were collected from the fish facility and transferred to a separate facility to avoid any contamination. One by one, fish were transferred to a tricaine bath (252 µg/ml). When the fish rolled onto their sides they were ready for injection. They were placed belly-up in a mounting sponge to hold the fish in place and to keep them moist. Injection was performed in the peritoneal cavity, just below the pelvic fin. The needle was inserted only so far in as to cover the beveled tip of the 27 G needle and approximately 10 µl of PBS or bacterial solution was injected. After injection the fish were transferred to a recovery tank before they were placed in new tanks with fresh water.

From there on the fish could be monitored for survival or be taken out for gene analysis at given time points, as described below.

3.5 Dissection of organs for gene expression analysis

In large, this procedure was executed as explained by Gupta et al. 2010 [118].

Shortly, the fish were euthanized with tricaine and pinned to the dissection plate on their side. The skin and muscle were then removed using dissecting scissors (Allgaier Instrumente, Frittlingen, Germany) and forceps (Dumont no5), to expose the internal organs. The organs of choice (spleen, liver, kidney and intestinal tract) were then removed and placed in an appropriate amount of RNAlater (as recommended by the manufacturer) and stored at 4°C until they were ready for use.

3.6 Enumeration of *M.marinum* from infected embryos

To determine the bacterial load during an infection, and eventual treatment, one can do a CFU enumeration. Embryos were selected at random.
The following protocol is an adaption of what is reported by Cosma et al. 2006 [115].

500 µl of embryo water with 20 µg/ml kanamycin was aliqouted into eppendorf tubes, one for each embryo. Infected embryos were transferred to one tube each and left to soak for 1 h at room temperature, this to reduce the contamination from normal flora. After an hour the embryo water was removed and replaced with 500 µl 200 µg/ml tricaine and incubated for 1 h on ice, this to euthanize the embryo. The tricaine solution was then removed and replaced with 150 µl 1x trypsin-EDTA (Sigma-Aldrich) and the samples were incubated for 1 h at 30°C. After an hour the embryos were homogenized with the use of a micropestle and returned to 30°C for half an hour more. After that, the samples were vortexed every half to whole hour; until there were no visible signs of embryo debris (takes 4 – 5 h).
When digestion was complete, 30 µl 1x PBS and 20 µl 1 % Triton X-100 (Sigma-Aldrich) was added to each tube and vortexed before they were placed in a water bath ultrasonicator for 10 min.
The samples were consolidated in a table top centrifuge before the entire volume, 200 µl (unless dilution series are needed), was spread evenly upon 7H10-kan agar plates supplemented with various antibiotics (amphotericin B, polymixin B sulfate, trimethoprim, carbenecillin (Sigma-Aldrich) to prevent the growth of contaminants from the embryo. Plates were incubated at 31°C until colonies could be seen (4 – 5 weeks), and they were subsequently enumerated using a stereomicroscope and cell counter.

3.7 Rifampicin and thioridazine bath experiments

RIF bath experiments

This protocol was adapted from the work done by Adams et al. 2011 [119].

For these experiments different concentrations of RIF (Sigma-Aldrich) were used: 100, 320, 500 and 640 µg/ml. Embryos were kept in petri dishes, which typically take 20 – 30 ml of liquid. RIF solutions were made for three days at a time, making the final volume 90 ml.

These experiments consisted of 8 groups in total (Figure 11).

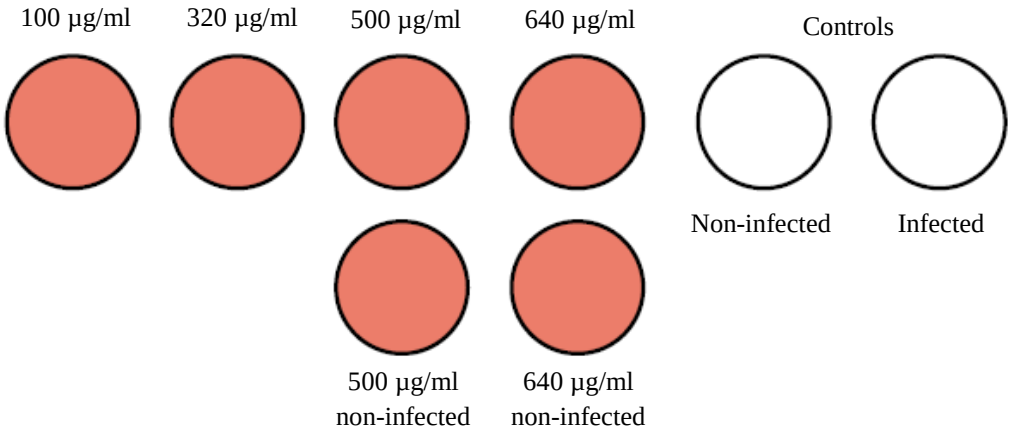

Figure 11: Schematic of experiment set-up.

RIF has low solubility in water and therefore had to be dissolved in DMSO (Sigma-Aldrich) (1 % of total volume) before adding it to the embryo water.

For three days one needs 90 ml RIF-water for the groups 100 and 320 µg/ml, subsequently 9 and 28.8 mg RIF was dissolved in 0.9 ml DMSO, respectively[4].
For three days one needs 180 ml RIF-water for the groups 500 and 640 µg/ml, subsequently 90 and 115.2 mg RIF was dissolved in 1.8 ml DMSO, respectively[3].

0.9 and 1.8 ml dissolved RIF was then added to 89.1 and 178.2 ml embryo water, to bring to a final volume of 90 and 180 ml, respectively.
Solutions were kept at 4°C and protected from light, as RIF is light sensitive.

[4] For calculations, see Appendix

Infected and uninfected embryos were transferred to the RIF baths 1 day post injection, dpi (3 days post fertilization, dpf), and the water was changed every day in combination with observing embryo survival.

TZ bath

The principle for this procedure is the same as described above, only TZ (Sigma-Aldrich) was used instead of RIF.

Again, 90 ml solutions were made, three days at a time with concentrations of 0.01, 0.05, 0.08, 0.1, and 0.5 µg/ml TZ. TZ is water soluble so 9, 45, 72, 90 and 450 µl of TZ stock solution (0.1 mg/ml), was each added to 90 ml embryo water.
Uninfected embryos were transferred to the TZ bath 3 dpf (the same time point as when the embryos were infected) and the water was changed daily while monitoring embryo survival.

RIF and TZ bath experiment

The principles are again the same as described earlier, the only difference is that here, RIF and TZ were used in combination (Figure 12).

One concentration of RIF was used, 320 µg/ml, and two concentrations of TZ, 0.01 and 0.1 µg/ml. With the addition of controls that makes 7 groups (Figure 12). The 90 ml solutions of 320 µg/ml RIF were made as described above, and the appropriate amount of TZ, also noted above, was added to the solutions.

Infected and uninfected embryos were transferred to the appropriate water baths 1 dpi/3 dpf, and the bath water was changed daily. Embryo survival was subsequently monitored.

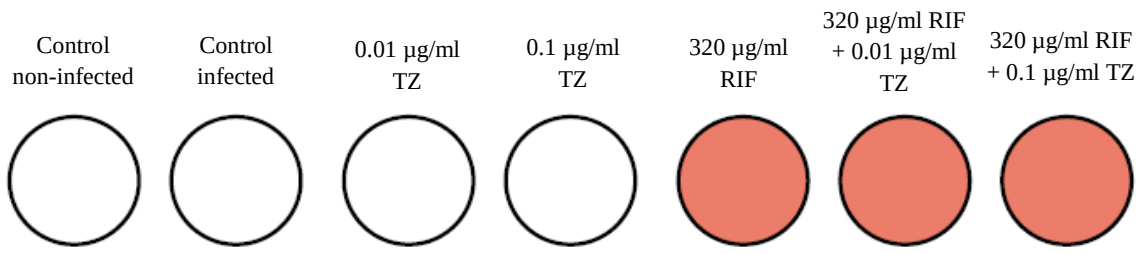

Figure 12: Schematic of experiment set-up.

Fluorescence imaging

Fluorescence imaging was performed on a Leica DM IRBE microscope (Leica, Wetzlar, Germany). Image processing was performed with the ImageJ software.

3.8 Nanoparticle preparation

Nanoprecipitation

First developed by Fessi et al. in 1989 [110], this method is relatively easy and it is performed in just one step (Figure 13).

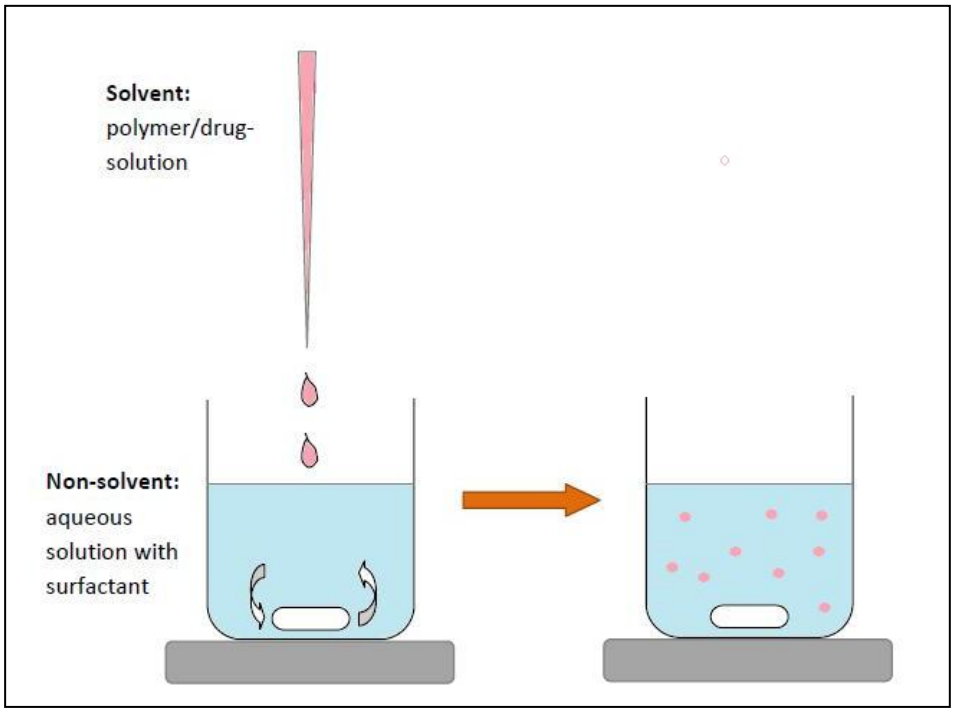

Figure 13: Nanoprecipitation procedure. The polymer-containing solvent is added drop-wise to the non-solvent and nanoparticles are formed immediately.

Because most polymers are water-insoluble, this technique is most suitable for encapsulation of hydrophobic compounds but many advances have been made in modifying the traditional method for use with hydrophilic compounds as well [88, 120].

Two miscible solvents are required; ideally the polymer and therapeutic agent of interest should be dissolved in one, the solvent; but not in the other, non-solvent. As soon as the polymer-containing solvent has diffused into the non-solvent medium, the polymer

precipitates, and drug entrapment is immediate. This phenomenon is called the Marangoni effect and particles with a size range of 100 – 300 nm are usually obtained. [120] Compared to emulsion-solvent evaporation techniques, nanoprecipitation is a mild technique. Here the shearing forces of homogenization and sonication can be avoided, a crucial factor when working with DNA and proteins.

The following procedure was adapted from the nanoprecipitation procedure described by Niu et al. 2009 [109].

Approximately 200 µg pDNA (pCMV-CAMP-GFP, Origene, Rockville, MD, USA) was taken out from a Maxiprep (Quiagen, Düsseldorf, Germany) solution and precipitated with the use of ethanol. Specifically, 5 µl 125 mM EDTA was added per 20 µl DNA solution. An appropriate amount of 96 % ethanol was added to create a 70 % solution and the sample was left to incubate on ice for 10 min. The sample was centrifuged at 6,000 x g, at 4°C for 30 min to pellet the precipitated DNA. The supernatant was then removed and the precipitated DNA could be used for encapsulation.
20 mg PLGA (Resomer RG 502H, Evonik Industries, Essen, Germany) and ~200 µg pDNA was dissolved in 1 ml DMSO and added to 20 ml 0.5 % Pluronic F-127 (Sigma-Aldrich) aqueous solution on a magnetic stirrer (600 rpm) using a syringe fitted with a 22 G needle at a speed of 0.5 ml/min. Nanoparticle formation is immediate, as can be seen by the milky blue color the solution obtains (Figure 14). The nanoparticle solution was left to stir for 5 h to facilitate the evaporation of DMSO.

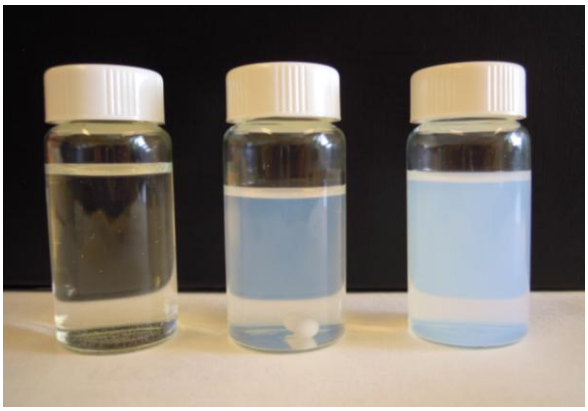

Figure 14: Successful nanoprecipitation can readily be seen by the milky blue color the solution obtains as more NPs are formed. To the left one can see water. The sample in the middle contains 20 mg PLGA-NPs and the sample to the right contains 40 mg PLGA-NPs. The intensity of color therefore increases with an increasing amount of polymer.

The nanoparticles can then be collected by centrifugation (25,000 x g, 4°C, 30 min) and subsequently freeze-dried or they can be concentrated with the use of centrifuge tubes fitted with filters (Spin-X UF, Corning Inc, Corning, NY, USA), at 9,000 x g for 30 min, and stored in aqueous solution at 4°C.

To make fluorescent particles, the same procedure can be followed only instead of pDNA, 0.05 mg of the fluorescent dye, coumarin-6 (Sigma-Aldrich), was added to the polymer solution prior to precipitation.

3.9 Nanoparticle characterization

Characterization and size estimation of the NPs was done by transmission electron microscopy (TEM) (Philips, CM100).

Before visualization, nanoparticles were adsorbed to a formvar/carbon-coated copper grid and subjected to negative staining.
The grids for electron microscopy were placed in a drop of the NP solution for 1 – 2 min and washed in distilled water three times before it was placed in a drop of 4 % uranyl acetate (Sigma-Aldrich) for 1 min. After incubation the grid was removed, excess liquid was removed with a filter paper and the grid was left to dry. When dry, imaging could be performed.

3.10 DNA extraction from NPs

To check the integrity of and to quantify encapsulated pDNA, the pDNA must be extracted from the NPs. This procedure was adapted from Niu et al. 2009 [109].

500 µl chloroform (VWR, BDH Prolabo, Lutterworth, England) was added to 100 µl concentrated NP solution diluted in 400 µl 1 x TE buffer. The solution was briefly vortexed before it was left to rotate end-over-end for 1 h at room temperature. After 1 h the solution was centrifuged for 20 min at 17,000 x g and the top, aqueous phase was collected for further analyses.

3.11 DNase I digestion analysis

NPs have been shown to protect encapsulated DNA from nuclease attack with the use of DNase I [104, 105]. This procedure is not only good for evaluating the protective abilities of NPs but also for the direct evaluation of whether or not the pDNA has been encapsulated at all. DNase I and the reaction buffer were acquired from the RNase-free DNase kit from Quiagen.

20 µl concentrated NP solution was added to 70 µl reaction buffer. 10 µl DNase I (~2.7 Kunitz units/µl) was then added to the sample and the sample was incubated at 37°C for 30 min. 10 µl 0.5 M EDTA, pH 8, was added to stop the reaction and the sample was incubated for 5 min at 65°C to inactivate the enzyme. This solution could then be used for subsequent analyses.

3.12 Analysis of DNA integrity

The following procedure was adapted from Niu et al. 2009 [109].

Extracted DNA was analyzed by gel electrophoreses on a 0.8% agarose gel.
0.4 g agarose (Invitrogen) was dissolved in 50 ml 1 x TAE buffer. Before casting the gel, 5 µl GelGreen (Biotium, Hayward, CA, USA) was added to the solution, as recommended by the manufacturer, to visualize DNA.
A 1-kb ladder (Invitrogen) was used and a 10 x loading buffer.
The gel was run at 90 V for 30 min and visualization was performed in a UV transilluminator (UVP, Upland, CA, USA).

3.13 Quantification of encapsulated DNA

To quantify the amount of DNA that is encapsulated, through DNA extraction, the PicoGreen (Invitrogen) reagent can be used. It is a fluorescent nucleic acid stain that binds double stranded DNA (dsDNA) and it can quantify as little as 25 pg/ml. The following procedure was acquired courtesy of Monica Hongrø Solbakken at Centre for Ecological and Evolutionary Synthesis, CEES, UiO.

To quantify the fluorescence from the PicoGreen reagent a FluoStar Optima (BMG Labtech, Ortenberg, Germany) microplate reader was used in addition to the Optima software. The microplate reader will apply 100 µl of the reagent to the wells for us but before one starts, one has to wash the system two times with distilled water.
A standard curve for the DNA solution needs to be made for every run, either the λ DNA supplied with the PicoGreen kit or preferentially the dsDNA one is quantifying. When using λ DNA a 2 µg/ml solution is made from the 100 µg/ml solution in the kit. Subsequently, concentrations of 1, 0.2, 0.02, 0.002 and 0 µg/ml are made to make up the standard curve and 100 µl of each is applied to a black 96-well plate (Greiner Bio One, Frickenhausen, Germany) in triplicate. All of these concentrations give us 200, 100, 20, 2, 0.2 and 0 ng DNA/well, respectively, and dilutions are made with 1 x TE buffer.
Before preparing the sample, it is beneficial to estimate the concentration of one's sample using Nanodrop or some equivalent, because the PicoGreen has an optimal binding range between 25 pg/ml and 1000 ng/ml.
The sample is diluted in 1 x TE buffer. The appropriate dilutions can range from 1:100 to 1:20,000, where the higher dilutions are more suitable for Maxiprep products. 100 µl of the samples are added to each well in triplicates.
The PicoGreen reagent should be diluted 200 x and enough solution should be made as to apply 100 µl to each well. In addition, one should account for the 1 ml needed to wash through the system before measurements are started. PicoGreen is light-sensitive and should therefore always be protected from light.
When ready, the microplate is put in the microplate reader, the system is primed once with TE buffer and once with the PicoGreen solution. When all settings are appropriate, measurements can start. The microplate reader applies 100 µl to each well, lets the reagent incubate for 5 min and measures the fluorescence.

The reader is saturated at 65,000 fluorescent units s^{-1} so measurements close to this value should be discarded. This means that the least diluted sample must be placed at the end of the reading as not to saturate the reader in the beginning and skew all subsequent readings. Measurements at 3,000 fluorescent units s^{-1} should also be discarded, as this is too low, measurements should preferentially be around 10,000.

3.14 Statistics

Statistics were performed on the survival experiments using the Minitab program (provided by the University in Oslo). A Log-rank test was done using Kaplan-Meier values to provide p-values, where $p < 0.05$ deemed the results significant.

4 Results

4.1 Zebrafish studies

As discussed earlier, *M.marinum*-infected zebrafish embryos have proven to be a good model system for *M.tb* infection in humans and the embryos will typically die from illness 6 – 8 dpi, depending on the bacterial load and individual susceptibility. The embryos' susceptibility to *M.marinum* infection is shown in Figure 15.

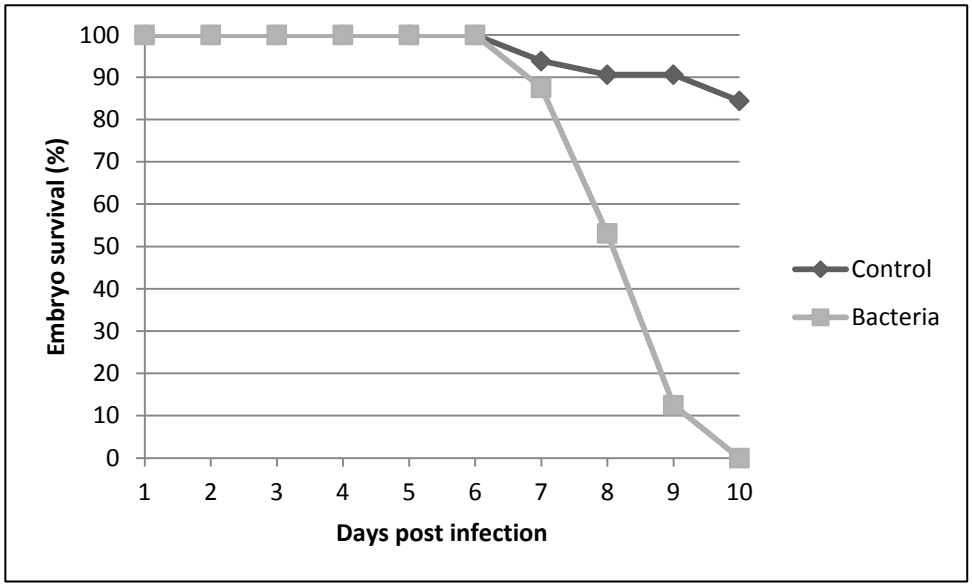

Figure 15: Survival experiment where embryos were infected with *M.marinum* at an OD_{600} ~ 0.8. Embryo survival started decreasing at day 7 and by day 10 all the infected embryos were dead. n = 32 per group. Data were deemed significant by a Log-rank test.

We also showed that the injection itself was not the reason for deaths among the embryos by injecting PBS in parallel with bacteria. The PBS injected group showed the same survival as the control group (data not shown).

4.1.1 Rifampicin bath treatment

In doing these experiments we wanted to establish which concentrations of RIF eradicate the bacteria and if toxicity would affect embryo survival. The following results were to help us get an idea of how much RIF we need to encapsulate and what amount of NPs need to be used in treatment, and subsequently what to expect from NP treatment.

Survival studies

Wild type zebrafish embryos were infected with *M. marinum*-DsRed at an OD_{600} of 0.962 (on average 25 bacilli per injection) 2 dpf and placed in baths containing different concentrations of RIF 1 dpi. Depicted in Figure 16 are the results obtained from one of the bath experiments, which I will subsequently refer to as experiment number 1.

The infected control and the 100 µg/ml groups could be found at the bottom of the graph with the lowest percentage of embryo survival over a period of 11 days of treatment. Indeed, 100 µg/ml RIF was a sub-optimal concentration and was not expected to facilitate a bactericidal effect. The 320 µg/ml group (MEC, minimum effective concentration[5] established by Adams et al. 2011 [119]) showed poor bactericidal activity with an embryo survival of approximately 30 %. The best therapeutic concentrations were 500 and 640 µg/ml, which showed approx. 50 % and 70 % embryo survival, respectively, and these groups were not significantly distinct from the uninfected control group. The 500 and 640 µg/ml uninfected control groups were also deemed non-significant by statistics, and together with the control group showed approx. 80 % survival.

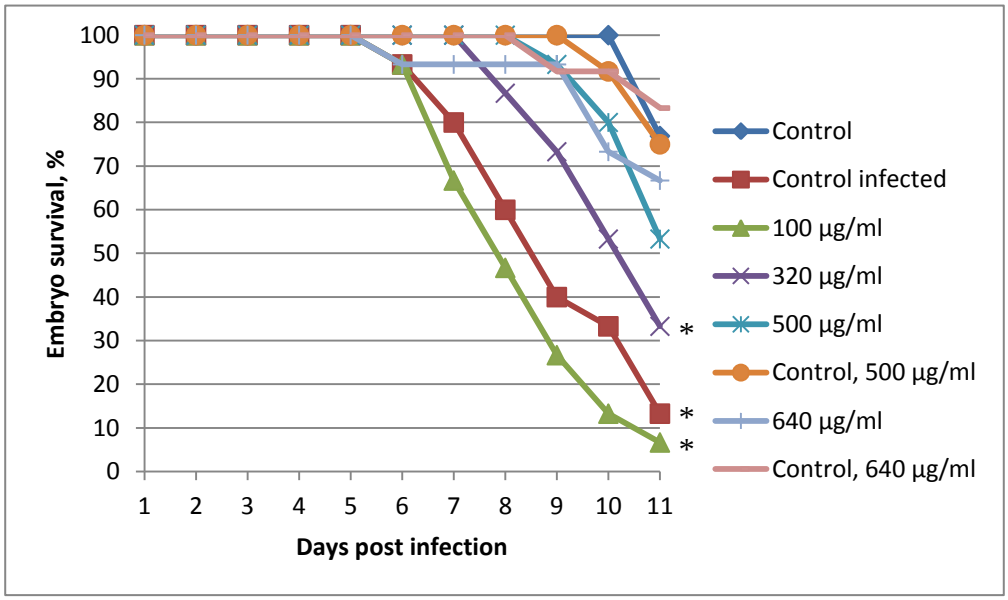

Figure 16: Survival experiment Nr. 1 with different concentrations of RIF. Asterisks mark groups that were deemed significant relative to the control group. Groups were of a size: $n \geq 12$.

The experiment was repeated, in the hope of being able to confirm the results obtained in this first experiment. However, this second experiment (experiment number 2) was not as

[5] Minimum effective concentration is the lowest concentration of drug that is non-toxic and normalizes host survival when administered to infected zebrafish embryos within 1 dpi [121].

successful as the previous one due to problems during the injection of bacteria. Clogging of the needle led to variable and lower bacterial loads. Even so, one could see the start of a similar trend as before, albeit later in the infection period (Figure 17).

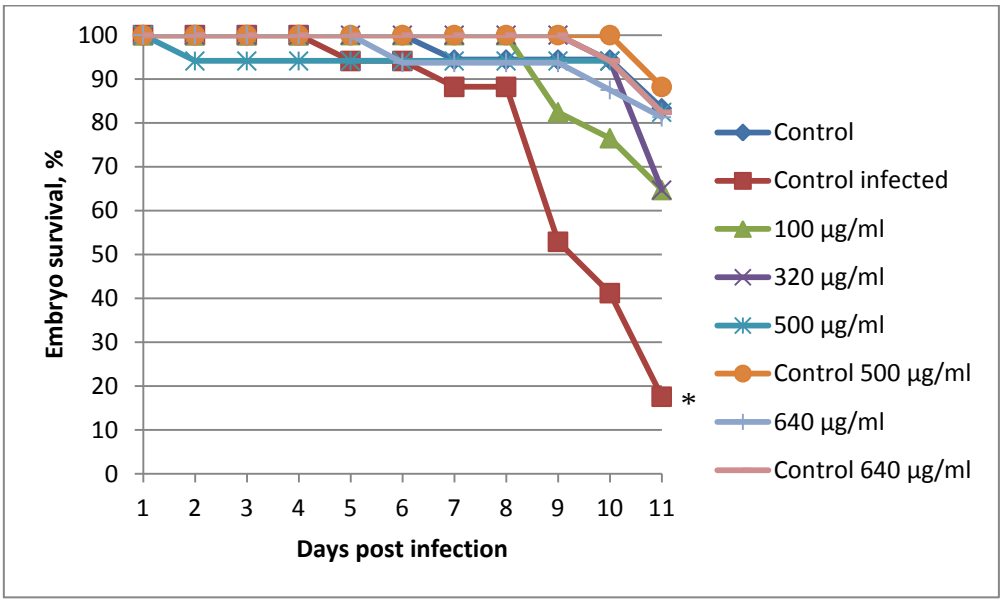

Figure 17: Survival experiment Nr. 2 in the presence of different RIF concentrations. WT embryos were injected with *M. marinum*-DsRed at an OD_{600} of 0.954. Groups had $n \geq 16$. Statistically significant groups are marked with an asterisk.

Also in this experiment the uninfected control groups showed 80 – 90 % embryo survival, together with the groups treated with 500 and 640 µg/ml RIF; again, there was no significant difference between the treated groups and the control group. The groups treated with 100 and 320 µg/ml RIF showed the same survival, ~65 %, and the untreated infected control group showed that only 20 % of embryos survived the 11 day monitoring period. The only group deemed significant in this experiment was the infected control group, making this experiment inconclusive, but I will later argue that a delayed trend could be seen in this experiment.

Fluorescence microscopy

In addition to monitoring survival, the bacterial load could be monitored directly using fluorescence microscopy (Figure 18). For every time-point: 3, 5, 7 and 9 dpi, three randomly chosen embryos were taken out for imaging. Imaging was performed on embryos from experiment nr. 2, where bacterial load was variable, but a trend could still be observed.

In Figure 18, one can see that in all groups the day 3 embryos did not show many bacteria. With this bacterial load, 3 dpi was too early to visualize granulomas but one could clearly see the increasing amount of bacteria over the days in fish from the infected control and 100 µg/ml groups. In the 320 µg/ml and 500 µg/ml groups, one could see that the load did not increase to the same level as the infected control group, but whether a plateau was reached or a decrease in bacterial load was achieved, was hard to say. At 9 dpi persisting bacteria could be seen in these two groups and in the 640 µg/ml group, but in the latter one had to look hard to find any bacteria.

Enumeration of bacterial load

A third way of monitoring infection was through CFU, where the infecting bacteria were isolated from tissue and plated so the colonies could readily be counted. The CFU results from experiment Nr. 1 are presented in Table 1, along with the standard errors.

Table 1: CFU from RIF bath experiment Nr. 1. Randomly, triplicates of embryos were removed from the experiment at the indicated time points and evaluated for bacterial load.

Days post infection	Infected	100µg/ml	320µg/ml	500µg/ml	640µg/ml
3	9±7	0±0	0±0	0±0	1±0
5	19±10	0±0	21±21	0±0	0±0
7	26±26	2±1	1±0	0±0	0±1
9	967±376	1350±1020	1±1	3±2	1±1

The CFU for the infected controls showed a steady, but low level increase over the experimental period, before it had increased dramatically by day 9. The 100 µg/ml group also showed a dramatic increase by day 9, but an increase during day 3 – 7 was not observed. The CFU for the 320 µg/ml group did not show the same trend as the infected group, and the results for 500 and 640 µg/ml were difficult to interpret, as too few bacterial colonies were observed to give us conclusive results. It is generally accepted that to obtain statistically valid data, the agar plates should contain between 30 and 300 colonies [62]; making these results inconclusive.

CFU was not obtained from RIF bath experiment nr. 2 due to the inconsistencies associated with this method.

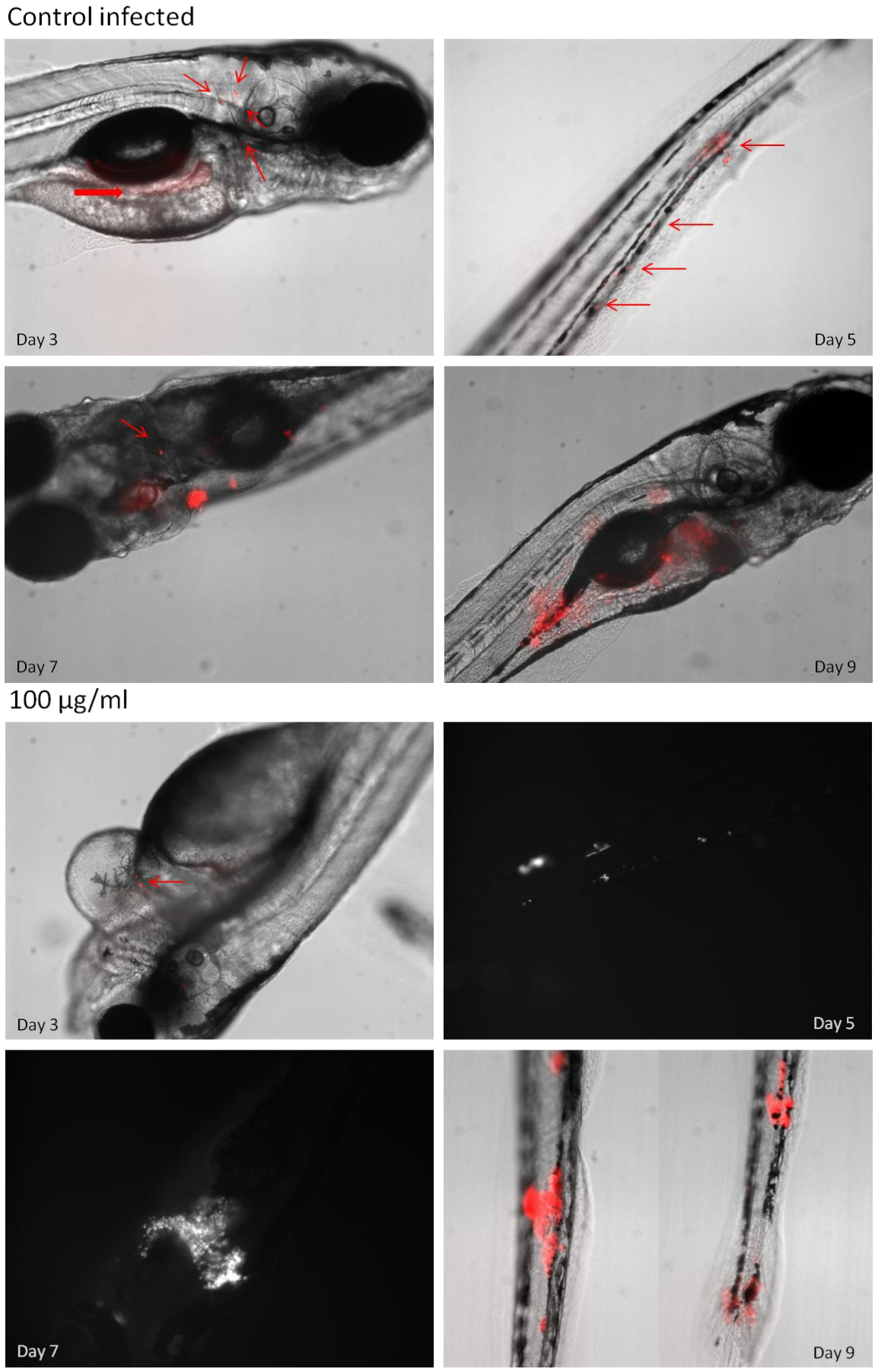

Figure 18: Visualization of bacterial load during infection with *M. marinum*-DsRed. Arrows indicate individual or small groups of bacteria. The thick arrow indicates auto-fluorescence of the intestine. Images were taken at 10X magnification.

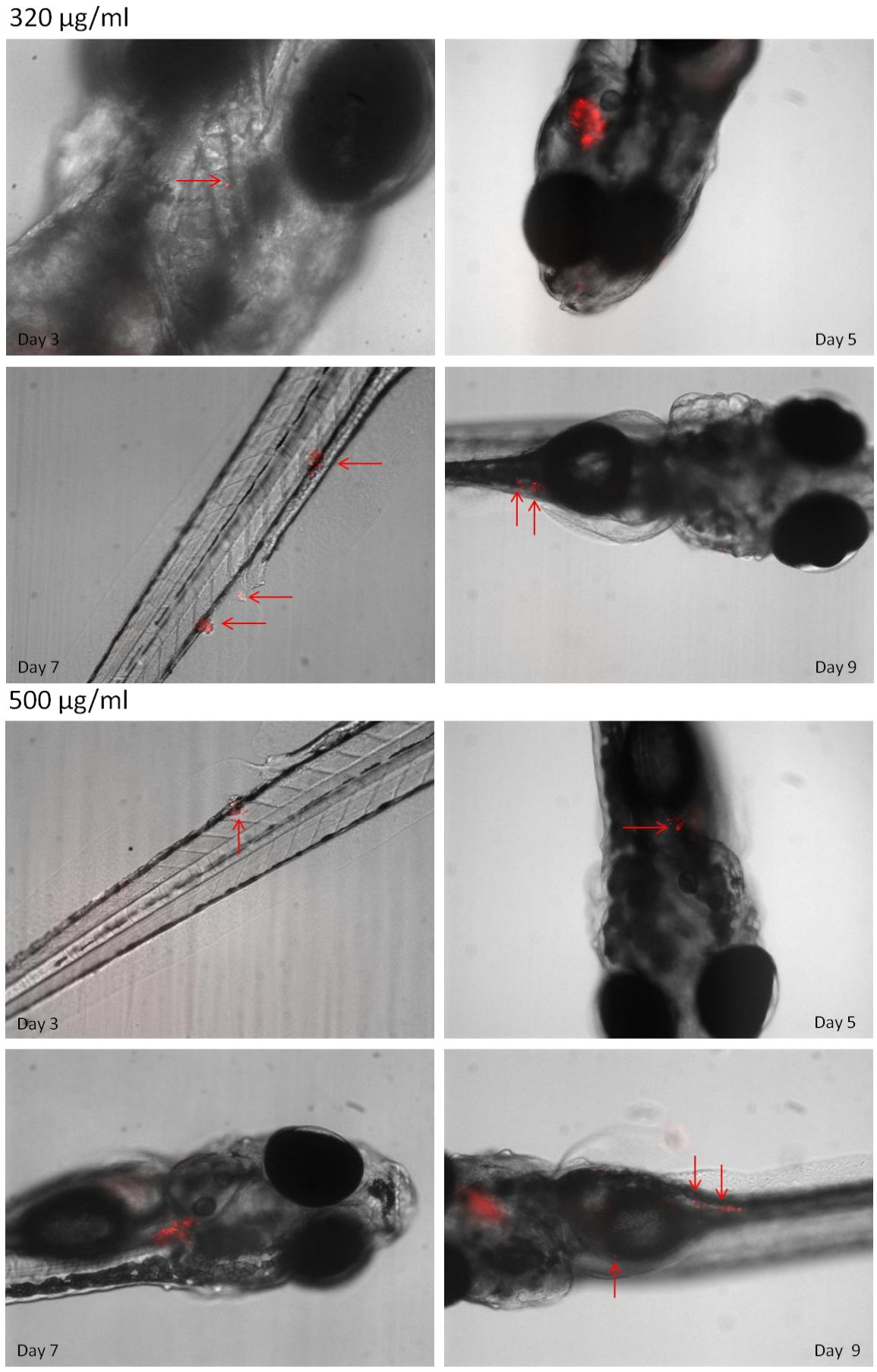

Figure 18: Visualization of bacterial load during infection with *M. marinum*-DsRed. Arrows indicate individual or small groups of bacteria. Images were taken at 10X magnification.

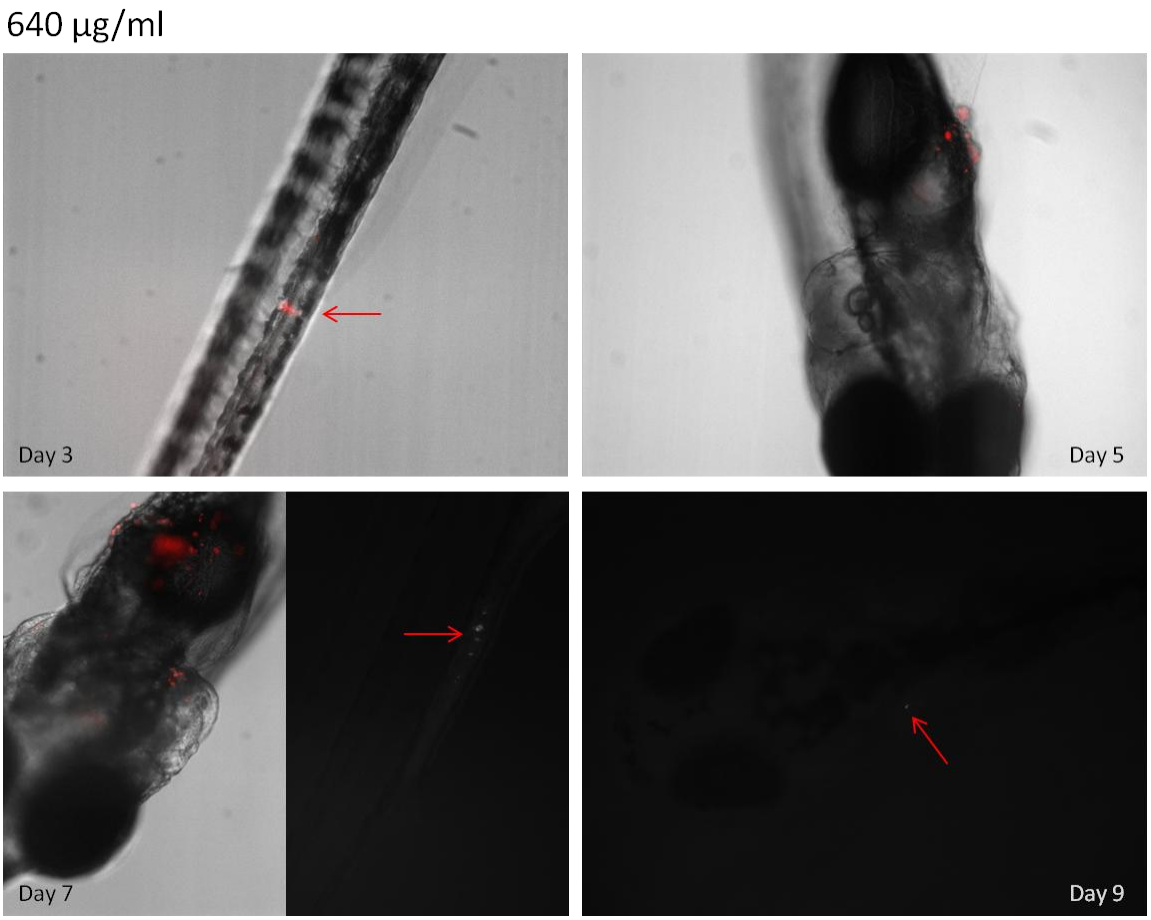

Figure 18: Visualization of bacterial load during infection with *M. marinum*-DsRed. In this figure we have a typical example of how different the infection can be in different individuals. In the left picture at day 7 one can see an abnormally high bacterial load, as opposed to the low bacterial load visualized in the picture to the right. Arrows indicate individual or small groups of bacteria. Images were taken at 10X magnification.

4.1.2 Thioridazine tolerance

Before we could use TZ in conjunction with RIF for the treatment of *M.marinum*-infected zebrafish embryos, the toxicity of this compound needed to be evaluated.

Wild type embryos were placed in water baths containing different concentrations of TZ, 3 dpf. As noted above, based on the results obtained from experiments with macrophages we knew that 0.1 µg/ml should be an effective concentration and we knew the upper limit would be 0.5 µg/ml, since this is the concentration used in treatment of psychotic disorders and we want to avoid possible effects on the central nervous system. During a pilot experiment it was observed that 0.1 µg/ml TZ had a toxic effect on embryos (results not shown), therefore lower concentrations were in addition chosen for this experiment.

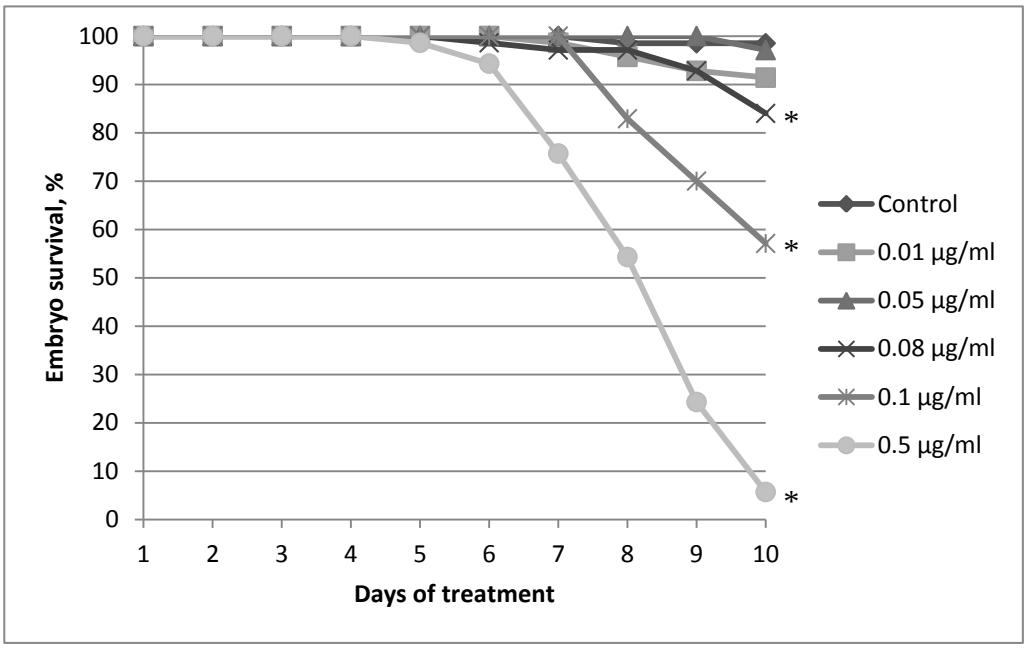

Figure 19: Toxicity of TZ monitored by survival. In contrast to the other survival experiments, the treatment period here is 10 days because a significant amount of controls died at day 11, leading to the exclusion of this time point all together. Asterisks mark the data determined to be significantly different from the control group. $n \geq 69$

As can be seen in Figure 19, 0.1 and 0.5 µg/ml TZ showed significant toxicity; ~40 % and >90 %, respectively, of the fish died during the 10 day monitoring period. 0.01 and 0.05 µg/ml TZ showed little to no toxicity but 0.08 µg/ml showed more toxicity, killing almost 20 %. The data for the 0.08 µg/ml group were deemed significantly elevated in comparison to the control group.

4.1.3 Rifampicin and thioridazine bath treatment

Based on the results obtained above we selected the concentrations 0.01 and 0.1 µg/ml TZ for more detailed evaluation. Even though 0.1 µg/ml showed significant toxicity, our rationale was that when encapsulated in NPs, the eventual goal, the toxicity would be predicted to be reduced since such treatment no longer is systemic but targeted.

Survival study

Wild type embryos were infected with *M.marinum*-DsRed at an OD_{600} of 0.8 and placed in treatment baths 1 dpi; the results are shown in Figure 20. As expected, the 0.1 µg/ml group showed significant toxicity. 0.01 µg/ml TZ showed no bactericidal effect as the group had approximately the same survival rate as the infected control group. Contrary to previous experiments, the 320 µg/ml RIF group showed very good bactericidal effect as its survival

was 80 %. Indeed, the data for this group was evaluated to be not significantly different from the control group. The embryos treated with RIF and 0.1 µg/ml TZ showed a survival rate of 40 % and the group treated with RIF and 0.01 µg/ml TZ showed a survival rate similar to the group treated with RIF alone and the control group. The difference between these two groups was not statistically significant.

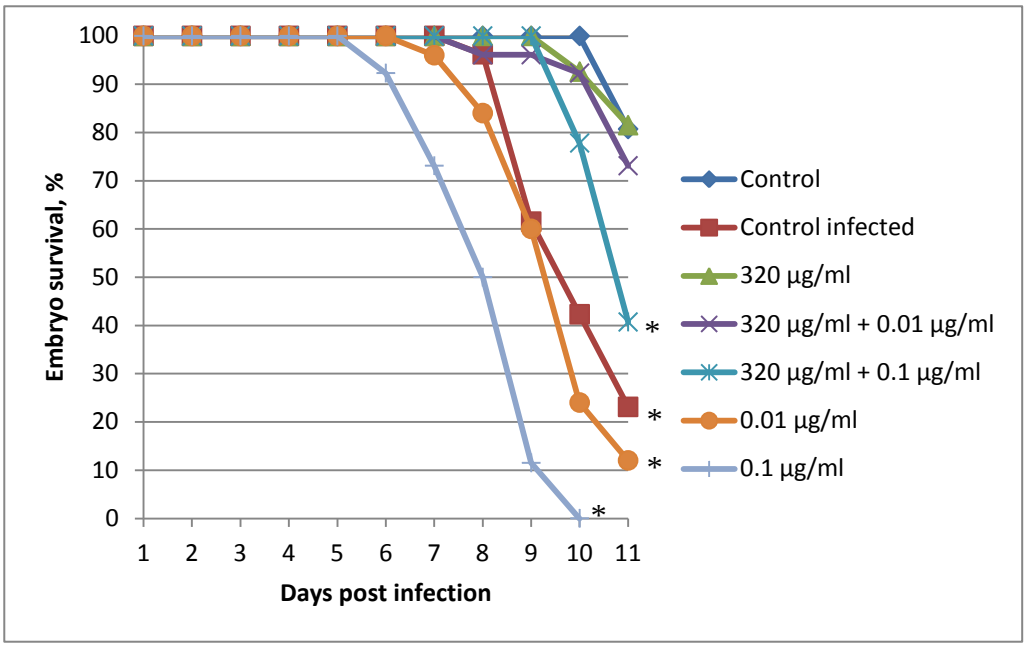

Figure 20: Survival experiment in the presence of RIF and TZ. Asterisks mark the groups that were determined to be significant in comparison to the control group by the Log-rank test. $n \geq 26$

Fluorescence microscopy

Also in this study, we monitored the infection visually by fluorescence microscopy. At the same time-points as before: 3, 5, 7 and 9 dpi, three embryos were randomly chosen for imaging. The images for the groups in this experiment can be found in Figure 21.

The infected controls showed a steady increase in bacterial load. The 320 µg/ml RIF group had some therapeutic effect, as seen earlier, but also here there was some variability as seen at day 9; when one embryo showed a higher bacterial load than the others. For the 320 µg/ml RIF + 0.01 µg/ml TZ group the same therapeutic effect could be seen as for the group treated with RIF alone, but when using 0.1 µg/ml TZ together with RIF the therapeutic effect seemed to be greater due to the presence of less bacteria at 9 dpi. Unfortunately, it was difficult to see the difference between the 9 dpi fish in the 320 µg/ml group with the least bacteria and the 9 dpi fish in the RIF + 0.1 µg/ml TZ group. The embryos treated with TZ alone did not show any reduction in bacterial load compared to the infected controls.

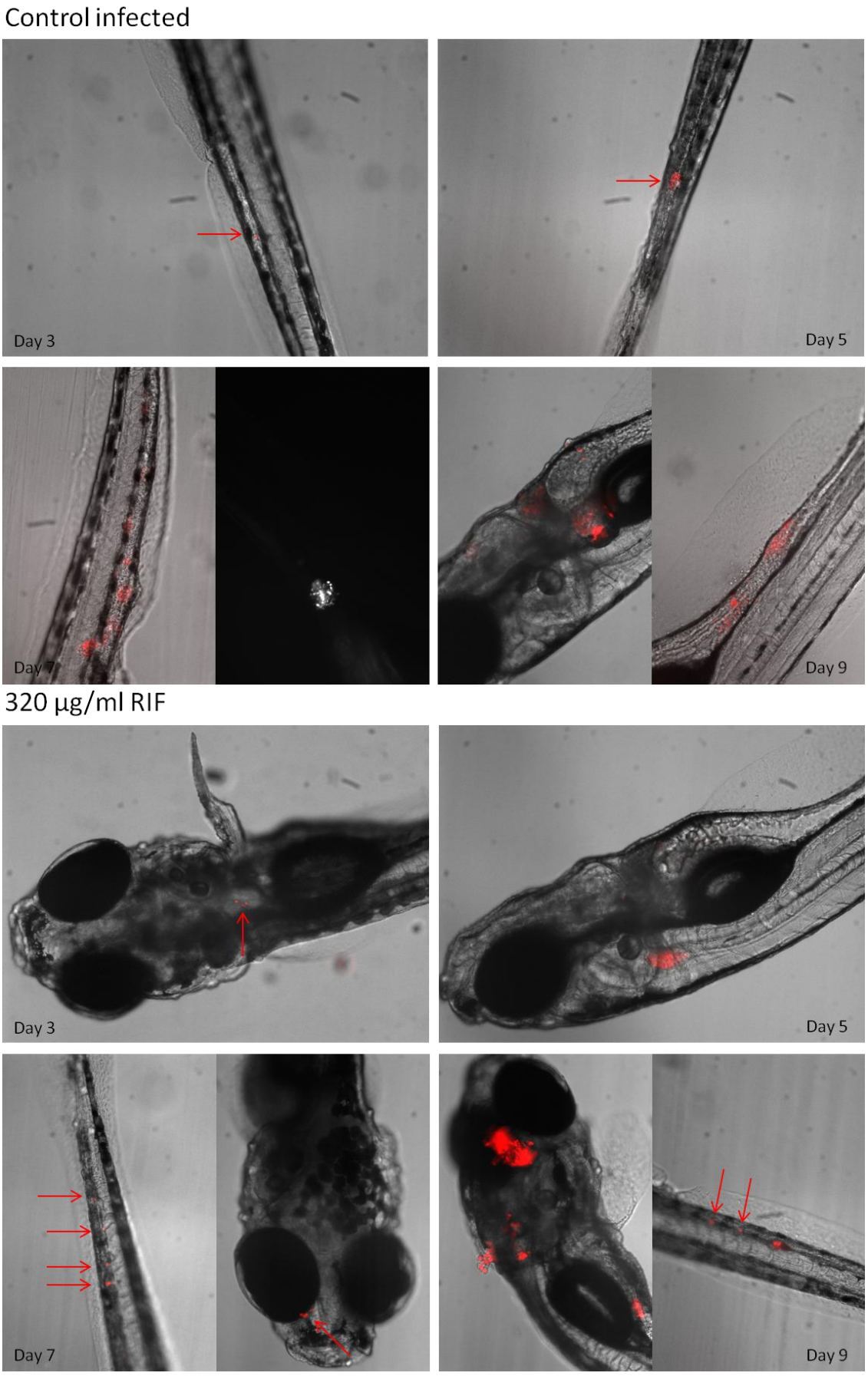

Figure 21: Visualization of bacterial load during infection with *M. marinum*-DsRed. Arrows indicate small groups of bacteria. Images were taken at 10X magnification.

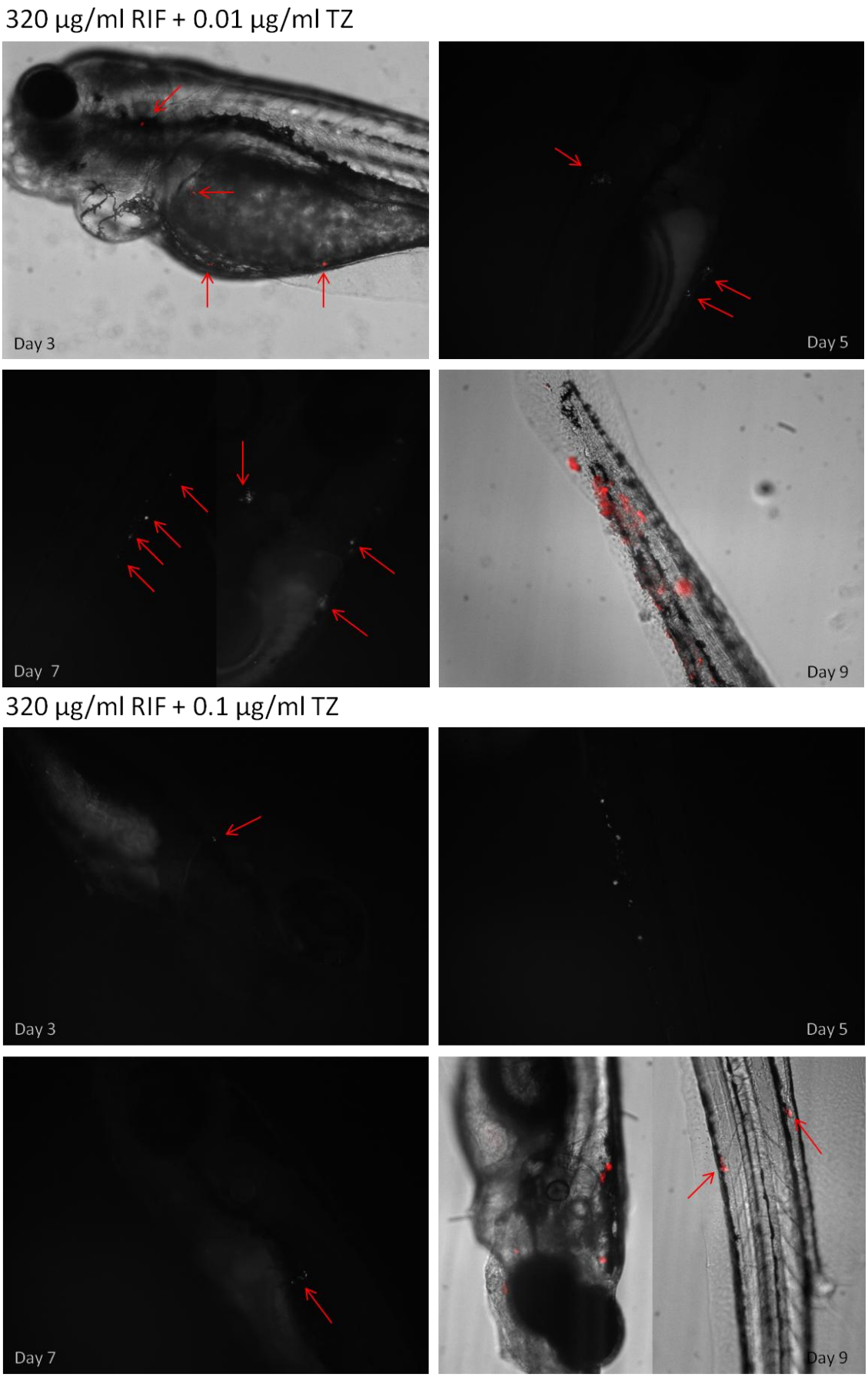

Figure 21: Visualization of bacterial load during infection with *M. marinum*-DsRed. Arrows indicate small groups of bacteria. Images were taken at 10X magnification.

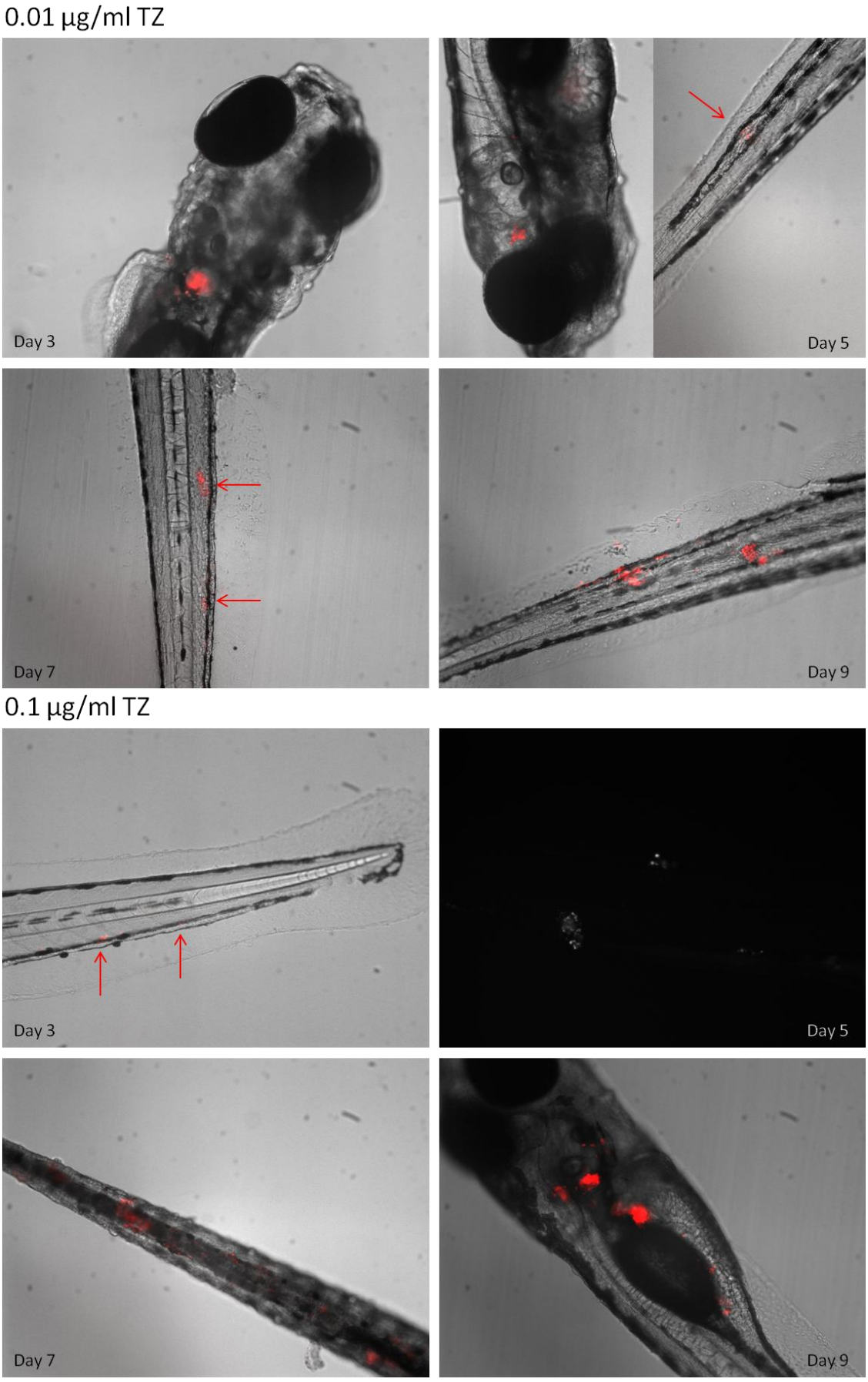

Figure 21: Visualization of bacterial load during infection with *M. marinum*-DsRed. Arrows indicate small groups of bacteria. Images were taken at 10X magnification.

4.2 Nanoparticles

In parallel to the experiments with antibiotics described above, we initiated a series of experiments aimed at encapsulating pDNA encoding an anti-microbial peptide in nanoparticles. In order to be able to monitor the uptake of the NPs into cells, and eventually into the zebrafish, we also decided to encapsulate a hydrophobic green-fluorescent dye, coumarin-6.

4.2.1 Increasing the average size of NPs

In our first attempt in making NPs, following the protocol reported by Niu et al. 2009 [109], we realized the particles were very small (Figure 22).

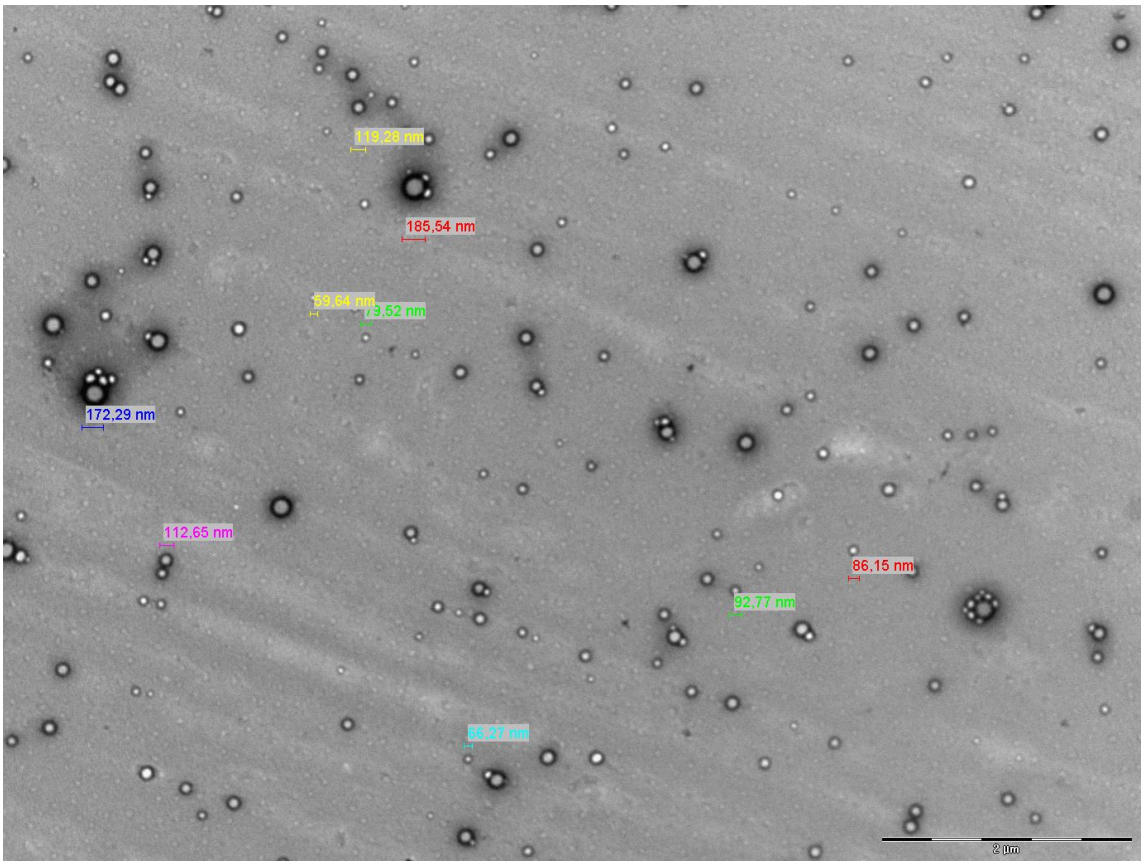

Figure 22: Electron micrograph of nanoparticles with sizes below 200 nm. Scale bar shows 2µm.

With the knowledge that macrophages preferentially phagocytose particles between 200 nm and 1000 nm and that this size range is the more effective for drug delivery, we set out to try to increase the size of the particles made by the nanoprecipitation method.

Several factors in the procedure could be altered to affect NP size: polymer concentration, solvent/non-solvent ratio, type of solvent or non-solvent, surfactant, stirring rate, drop size and eventually drug to polymer ratio. One by one these factors were altered in the attempt to make bigger NPs and the results are listed in Table 2.

Table 2: Size range was estimated by measurement of particles in randomly chosen spots on the grid.

Batch	Non-solvent	S/NS ratio	Polymer conc. (mg/ml)	Pluronic F-127 (%)	Rpm	Size range (nm)
1	H_2O	0.05	20	0.5	600	50 - 170
2	H_2O	0.05	40	0.5	600	80 - 150
3	H_2O	0.05	20	0.5	450	50 - 120
4	H_2O	0.05	40	0.5	300	70 - 200
5	H_2O	0.05	40	0.5	100	70 - 180
6	H_2O	0.05	20	0.25	300	90 - 170
7	H_2O	0.05	20	-	300	70 - 130
8	H_2O	0.025	40	0.5	600	80 - 140
9	H_2O	0.25	20	0.5	600	80 - 160
10	H_2O	0.1	20	0.5	600	30 - 125
11	Ethanol	0.05	20	-	600	70 - 200
12	Ethanol	0.05	20	0.5	600	50 - 160
13	H_2O	0.05	20	1 (PVA)	600	60 - 115

As one can see above, changing these factors had little to no effect in producing sizes above 200 nm. The one factor that stayed the same, the solvent, may be the factor that could effectively increase NP size. However, due to the fact that we were trying to encapsulate pDNA, we were limited to the use of DMSO so as not to compromise the delicate nature of DNA when associated with organic solvents. The fluorescent compound coumarin-6 is hydrophobic, so organic solvents could safely be used for its encapsulation. When DMSO was used as the solvent, particles with sizes similar to the ones presented in the table above were produced: < 200 nm, but when acetonitrile, MeCN, was used as the solvent, bigger particles were obtained; 50 – 320 nm (Figure 23).

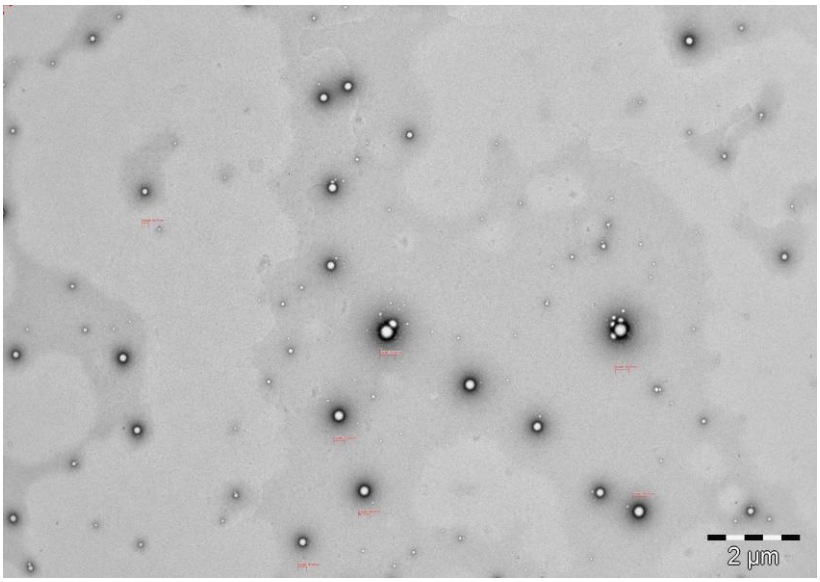

Figure 23: Coumarin-loaded NPs made with MeCN as solvent produced NPs up to 300 – 400 nm in size. Scale bar is 2 µm.

4.2.2 Encapsulation of pDNA

Even though we failed to acquire NPs in the preferred size range, we continued our endeavor to encapsulate pDNA with the nanoprecipitation method. For encapsulation, a pCMV-GFP vector with the human cathelicidin, LL-37, as insert was used. If successful, GFP expression could then be monitored *in vitro* in BCG-infected macrophages and subsequently the effects of LL-37 expressed via the pDNA could also be monitored in both macrophages and zebrafish through the reduction in bacterial load.

The first challenge we encountered was dissolving the DNA in DMSO. After performing a Mini- or Maxiprep, the extracted pDNA was eluted preferentially in water or TE-buffer. Mixing this solution directly with DMSO led to a reduction in the solution's hydrophobicity and PLGA would therefore not dissolve properly, leading to failed nanoprecipitation. The appropriate amount of pDNA was therefore precipitated with ethanol to allow direct dissolution of the pellet in DMSO. We soon realized the pellet was hard to dissolve in DMSO alone so we started to dissolve the pellet first in 30 µl TE-buffer, pH 8, and then add the 1 ml of DMSO. With this procedure, the nanoprecipitation was successful but we then had to determine whether the pDNA was actually encapsulated or if it was free in solution. In Figure 24 one can see that pDNA was present in the NP solution, both before and after DNA extraction with chloroform.

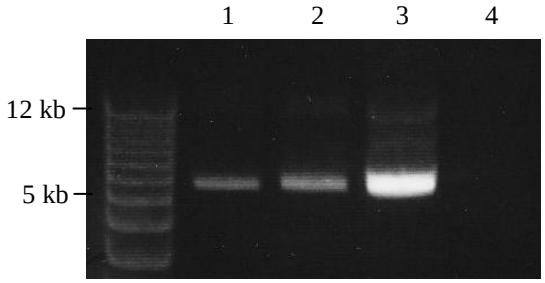

Figure 24: Agarose gel electrophoresis of pDNA-NPs and extracted pDNA. Lane 1 contains the pCMV-CAMP plasmid (7.1 kb) as a positive control. Lane 2 shows the extracted pDNA and lane 3 shows the pDNA-NP solution from which pDNA was extracted. Lane 4 contains a solution of empty NPs as a negative control.

Seeing that these results did not unequivocally tell us whether the pDNA was inside or outside our NPs, we used DNase I to eliminate potential non-encapsulated pDNA in the solution. The results revealed that, in fact, no pDNA could be extracted from the DNase I treated pDNA-NP solution, arguing, to our disappointment, that no pDNA was encapsulated (results not shown).

Because of its hydrophilic nature, it was clear that DNA would rather be in water than in DMSO. We considered the possibility that the small amount of TE-buffer used to dissolve the DNA may have compromised the encapsulation process. We therefore sought to eliminate aqueous solutions from this step all together. We then went back to the original strategy of trying to dissolve the pDNA pellet directly in DMSO by heating the solution up to approximately 50°C during magnetic stirring. The pellet seemed to dissolve and the nanoprecipitation was successful. The results of DNase I treatment of these NPs can be seen in Figure 25.

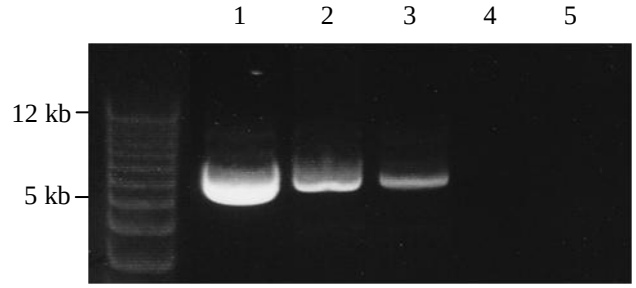

Figure 25: Agarose gel electrophoresis of DNase I treated pDNA-NPs and extracted pDNA. Lane 1 contains the pCMV-CAMP plasmid as a positive control. Lane 2 shows the pDNA containing NP solution and lane 3 contains the extracted pDNA from that sample. Lane 4 contains pDNA-NP solution that has been treated with DNase I, and lane 5 shows the extraction product from that solution.

As shown in Figure 25, no pDNA could be detected in the DNase I treated pDNA-NPs, showing again that pDNA was not successfully encapsulated. To our disappointment, this problem remains to be resolved by others in our group.

4.3 Gene expression analyses

Gene expression analyses were performed on both infected embryos and adults for NK-lysins 1-4 but the results from both preliminary experiments were highly inconclusive. The inconsistencies observed in both the infected and uninfected groups lead to a halt in further analysis.

5 Discussion

In this thesis I took advantage of the zebrafish-*M.marinum* model system established by the Ramakrishnan group in order to initiate a series of experiments aimed at improving therapy against *M.tb*. Our group has recently established the use of PLGA-NPs loaded with the antibiotic rifampicin (RIF). These NPs have been used to treat BCG-infection in macrophages and *M.marinum*-infection in zebrafish embryos to such a degree as to clear the infection (Kalluru et al. in prep., Fenaroli et al. work in progress). My strategy in advancing this progress was two-sided. First, I initiated experiments where the effects of the antibiotic RIF and the efflux pump inhibitor TZ, both alone and in combination, were examined in *M.marinum*-infected zebrafish embryos. The rationale here was that TZ would work in synergy with RIF to more effectively decrease, and hopefully eradicate, the bacterial load during infection. Second, given the increasing difficulty to treat drug-resistant *M.tb* strains, I sought to develop an alternative strategy: to deliver pDNA encoding anti-mycobacterial peptides to mycobacteria-infected cells.

5.1 Antimicrobial peptides as therapy against *M.tb*

Experimental work with peptides is expensive and the yield from production is usually low [16]. In addition, many exogenous peptides are sensitive to the physiological salt concentration in our bodies [18]. Thus, their short half-lives and toxicity [16], led us to prefer the idea of using pDNA encoding the peptides of interest for therapeutic studies. Amplification of the pDNA is cheaper and easier, and high yields can be obtained with the use of Maxi- or Giga-preps. Once expressed at the target site, the antimicrobial peptides present many theoretical advantages over antibiotics, as mentioned earlier. Briefly, those advantages include: activity against many different bacteria, including those that are drug-resistant, and the unlikely acquirement of resistance.

Four peptides were considered for use in therapy against *M.marinum* in zebrafish embryos: defensins, cathelicidin, NK-lysin, and Ci-MAM-A24. All of these show bactericidal effects against *M.tb*, making them good candidates for use [18, 25, 36]. A lot of thought was put into which peptides should be used in the beginning of my project and eventually we decided to use a commercially available construct for proof of principle; the pCMV-CAMP-GFP construct that contains the human gene for the cathelicidin, LL-37. Even though the peptide is

not native to zebrafish, we believe the peptide should still work as an anti-mycobacterial agent due to its known activity. LL-37 has been reported to be expressed in many different cells during *M.tb*-infection, where the highest levels were reported in alveolar macrophages [35]. This suggests that LL-37 plays an important part of the host's defense against *M.tb*, and that increased presence of this peptide facilitates the killing of this pathogen. Thus, I expect that all anti-microbial peptides that show killing activity against *M.tb* should be effective whether they are native to the host organism or not.

5.2 Nanoparticle-based therapy

We believe that NP-based therapy will become increasingly important in future medicine and that this will help us overcome many of the obstacles in traditional medicine we are faced with today. As mentioned earlier, toxic side-effects, development of resistance, length of treatment, and frequency of dosing, are all negative features associated with TB treatment [6, 87]. We believe all these characteristics can be avoided with the use of drugs encapsulated in NPs, as opposed to the free form (oral, injection, and aerosol). Indeed, results have shown that this is exactly what is achieved when using RIF-loaded NPs in treatment of TB. NPs are transported to the site of infection (no targeting is necessary since macrophage uptake is the default pathway) and will lead to a higher local concentration of drug [95]. This in turn prevents systemic toxicity and can prevent the emergence of drug resistance, while the length of treatment and the dosing frequency can be drastically reduced [97, 99], leading to lower costs for this treatment regimen.

We are in the process of using RIF-NPs for the treatment of BCG-infection in macrophages and *M.marinum*-infection in zebrafish embryos, but we are also pursuing the possibility of encapsulating other anti-mycobacterial compounds, such as TZ and plasmid DNA that encodes anti-microbial peptides. We think that the use of RIF-NPs in combination with NPs loaded with additional anti-mycobacterial compounds could be a promising solution to effectively eradicate a mycobacterial infection.

Concerning TZ, we believe the toxic side-effects that are often observed with this compound can be largely avoided by encapsulating the drug in NPs. These NPs would then deliver TZ directly to macrophages, as it does RIF, and targeted and sustained release would prevent the systemic spread of the drug.

DNA-NPs can improve two important aspects as opposed to using naked DNA in therapy: (1) they can transport intact DNA across cell membranes and epithelial layers, and (2) the polymer of the NPs protect the DNA from nucleases [104]. As macrophages have proven difficult to transfect with standard DNA transfection procedures, NPs offer an attractive alternative for transfection. Macrophages are thought to most efficiently phagocytose particles between 200 and 1000 nm [9]; a fact that led to the work I put in to increasing the size of the particles I produced. If the particles are smaller than 200 nm, we expect phagocytosis to not be as effective due to the small surface area receptors have to bind, making the signal for phagocytosis weak. Unfortunately, I had no success in achieving this goal, despite considerable efforts. Even though there are many papers that give instructions on how to achieve the optimal size and drug loading, I was unable to overcome the problem of small size. For some reason I cannot explain, I was not successful in increasing the overall size of the particles. Nevertheless, in parallel I continued with my work to encapsulate pDNA.

5.2.1 Making plasmid-DNA loaded nanoparticles

Following my discovery of a paper by Niu et al. [109] where pDNA is encapsulated into PLGA-NPs by the nanoprecipitation method, I immediately wanted to try this for myself. Not only was the method simple, but the DNA would not be subjected to the detrimental effects of sonication. It turned out that the major problem associated with this procedure was dissolving pDNA in the solvent, DMSO. In that paper, it was actually not mentioned how DNA is dissolved in the DMSO solution, so the procedure that group used remains unclear to us. Nevertheless, we sought to solve the problem ourselves, and what we achieved was visible dissolution of the pDNA pellet in DMSO through heating and stirring. It is quite possible that the pelleted pDNA was not completely dissolved at the moment the solution was used for nanoprecipitation, even though it was perceived as so. I imagine that if the pDNA is not completely dissolved in the solvent, the molecules will preferentially aggregate and encapsulation will not be successful, leading to the escape of pDNA into the non-solvent, water.

As this is the only report of pDNA encapsulation using the nanoprecipitation method, there is not much help to be found in the literature. This may be a sign that this method is not reproducible, or that further optimization (not mentioned by Niu et al.) is required.

Nonetheless, my work lays the foundation to find new ways of solving this problem in the Griffiths group. In addition, the establishment of the protocols for NP preparation by nanoprecipitation and characterization of pDNA integrity will help these future experiments.

5.3 Rifampicin as a therapeutic agent against *M.marinum* in zebrafish embryos

Throughout this thesis, the focus on RIF is related to its crucial role in the treatment of TB in humans. As *M.marinum* is also susceptible to RIF [121, 122], one could deduce that the same principles in treatment apply. The MIC[6] (minimum inhibitory concentration) and MEC for RIF against this particular strain of *M.marinum* has been established by Adams et al. 2011 [119] to be 0.32 µg/ml and by Cosma et al. 2006 [123] to be 320 µg/ml, respectively. These are the data my experiments are based on.

Relevant for my results are the results obtained by Adams et al. 2011 [119]. Some key points from that paper include:

- Continuous treatment of infected embryos with RIF MEC led to a survival rate similar to uninfected controls and a 3-day treatment with two times the MEC lead to an increased reduction in bacterial load, despite its toxicity (measured by fluorescence microscopy).

- Drug-tolerant bacteria persist in infected zebrafish embryos, and they appear early in infection.

- Development of drug-tolerance depends on macrophage residency and presence of the drug.

- Drug-tolerance is mediated by efflux-pumps and the addition of inhibitors towards these pumps leads to a reduction in bacterial load.

Keeping these issues in mind we chose to use four different antibiotic concentrations to evaluate the treatment of *M.marinum*-infected zebrafish embryos through bath treatment: the RIF MEC (320 µg/ml), a sub-optimal concentration (100 µg/ml) and two concentrations

[6] Minimum inhibitory concentration is the lowest concentration of drug that visibly inhibits bacterial growth *in vitro*.

above MEC (500 & 640 µg/ml). Since RIF has dose-dependent activity [119, 124], it would be interesting to observe if bacterial clearance could be achieved more rapidly at doses higher than the MEC.

Rifampicin bath experiments

Looking at Figure 16, one can see a clear trend: the higher the concentration of RIF, the higher the embryonic survival. This trend can likely be explained by the bactericidal activity associated with RIF. The infected control group shows the expected mortality and this is supported by the CFU results (Table 1). Also expected was the high mortality observed for the 100 µg/ml group, since this is a sub-optimal concentration of RIF. Considering the results for the 100 µg/ml group, it appears that this sub-optimal concentration actually increases virulence, possibly by the emergence of more tolerant bacilli. These results from the survival experiment are, in comparison to the infected control group, not fully supported by CFU results; the exception being the results from 9 dpi, where a CFU of 1350 fits well with the fact that this group of embryos showed higher mortality than the infected control group. The MEC group (320 µg/ml) in this experiment shows poor bactericidal activity, as compared to the results presented by Adams et al. 2011, where 320 µg/ml normalizes embryo survival. The reasons for this may be a higher amount of tolerant bacteria or increased host susceptibility to the infection. The groups treated with 500 and 640 µg/ml were all determined to be statistically non-significant relative to the control group, indicating that therapy was successful and that, visually, toxicity was not a problem.

Figure 17 does not show a clear trend, but this could be explained by the clogging of the needle during injections. Thus, the bacterial load was expected to be quite variable and lower than in experiment nr. 1. In looking at the infected control group in Figure 17, one can clearly see that the infection is delayed by 2 days when comparing it to experiment nr. 1 (Figure 16). The mortality in the infected control group started at 6 dpi in experiment nr. 1, while it began at 8 dpi in nr. 2. One could therefore argue that the results seen for the other groups were also delayed by 2 days. Moreover, if the experiment could have progressed longer, we might have seen results more similar to the first experiment. The reason for this limited time period of 11 dpi is that at this time the embryos were 13 days old and were not fed during the course of the experiment, so at this time, non-specific deaths started occurring.

Although one could question whether this second experiment is reliable at all, the images in Figure 18, taken of randomly chosen embryos, show clearly that an infection has been initiated and is progressing. From my experience I can say that these images reliably represent how a typical infection progresses with the only difference being the initial bacterial load and, therefore, how long the embryos survive. The data for the infected control group were the only ones determined to be statistically significant by a Log-rank test. Even so, I would argue that we can see the beginning of a decreasing survival trend in the 100 and 320 µg/ml groups ($p = 0.087$ and $p = 0.103$, respectively, when compared to the control group) at the last time point and that if it were possible to continue the experiment, the decrease would be greater over time. The images in Figure 18 support this hypothesis. A steady increase in bacterial load was observed for both the infected control and 100 µg/ml groups. The same increase was not observed in the remaining groups due to the bactericidal effect of RIF, but persisting tolerant bacteria were observed. The therapeutic effect is especially clear in the images for the 640 µg/ml group, where at 9 dpi, bacteria were very hard to find or could not be found at all. At 7 dpi different bacterial loads were observed, some with a significant amount of bacteria and others with hardly any bacteria at all; the latter is consistent with the images from 9 dpi. It is important to note that when dealing with a system like this, where multiple individuals are used to test the effects of a drug, there will be some inherent biological variation in the results. Some may be more susceptible to the infection and others may be quite capable to decrease the bacterial load on their own. Due to the clear trend presented in the image analysis one can say that the conclusions made here represent the majority.

In comparison to Adams et al. 2011, the results obtained here were quite different. They reported 100 % mortality of uninfected embryos treated with two times the MEC, i.e. 640 µg/ml, within 6 days of treatment. This finding is not supported by my results as the difference between the 640 µg/ml groups and the control groups in both experiments (most importantly in the first due to the higher bacterial load) was determined to be non-significant by statistical analyses. At the most, approximately 30 % mortality was observed for this group over a period of 11 days. I cannot claim that the embryos experience no toxicity at all, but based on my results, I can safely claim that this concentration will not kill them.
As for the MEC groups, different survival was observed in the two experiments; 30 % survival for experiment nr. 1 and 60 % for nr. 2. In the former, the survival declines from 70 to 30 % in two days, making it reasonable to suggest that if it had not been for the 2-day delay, similar results would have been obtained. Either way, these results differ greatly from

the results reported by Adams et al. where by 11 days of treatment, 70 – 80 % of infected embryos were still alive. The reason for these different results is hard to interpret, since the same strains of *M.marinum* and zebrafish were used. The differences, therefore, must lie in the experimental design. For example, we inject approximately 25 bacilli, determined by CFU, while they report infection with 800 bacilli, estimated by a procedure that is not evident in their publication. Even so, the infected control groups in both experiments experienced mortality around the same time; day 6 – 7, but compared to my results, the decline in survival is steeper in the data presented by Adams et al. 2011. Therefore, it could be possible that the amount of bacteria injected does not significantly affect the rate of killing in zebrafish embryos in the range between 25 – 800 bacilli, or that different methods are used to estimate this amount of bacteria, but as this is not mentioned by Adams et al. it is hard to say.

Obviously these experiments need to be repeated as completely reproducible and interpretable results were not obtained, but my data agree with some of the data presented by Adams et al. 2011 in that tolerance towards RIF plays a significant role in treatment failure. This can be stated because *M.marinum* growth should be inhibited by RIF, as proven *in vitro* [123], but as shown by Adams et al. 2011, this is not the case *in vivo*. The bacterium has developed a system where the effects of antibiotics can be circumvented by up-regulation of efflux pump numbers or activity. This transient phenotypic change is called tolerance. Creating a treatment strategy where inhibitors towards these pumps are used in combination with antibiotics provides an attractive strategy to focus on in future experiments. In addition, with the use of RIF loaded NPs, a therapeutic concentration can be achieved inside the macrophage (the site of infection), possibly circumventing this problem all together. This is something that needs to be further evaluated in the future.

CFU enumeration

In addition to the fact that counts below 30 are statistically unreliable when doing CFU [62], I suspect that there may be a threshold for detection; thus, when one's counts are below a certain number, the variability in the number of colonies that form is very high. This seems to be the case for the 500 and 640 µg/ml groups and is probably one of the main flaws of CFU enumeration. The low counts observed in the results presented (Table 1) can also be due to errors performed during the process, such as inconsistent pipetting or more likely, failure to homogenize the sample completely and clumping of the bacteria. Since *M.marinum* naturally

clumps in culture it is not unreasonable to think that this could be the case because if two or more bacteria are clumped when plated, only one colony will arise. And it is important to keep in mind that we are counting colony forming units, not all viable bacterial cells. The CFU will therefore always be an underestimate of the true number of viable bacteria.
I conclusion, I would say that this method needs to be further optimized. This is underscored by the fact that no CFU results were obtained from experiment nr. 2 and that it takes more than 1 bacterium to induce the mortality observed for the 320 µg/ml group in Figure 16.

5.4 The effect of thioridazine on bacterial load

As explained earlier, TZ has great potential as a therapeutic agent against mycobacteria; both alone and in concert with antibiotics. Since Adams et al. 2011 reported that tolerance towards antibiotics is induced by efflux pumps and that efflux pump inhibitors reduced the bacterial load even more than with antibiotics alone, the thought of using an efflux pump inhibitor in combination with an antibiotic to eradicate a mycobacterial infection has been a compelling idea. We therefore sought to try a combination of TZ and RIF in the *M.marinum*-zebrafish model system.

We found that above a certain concentration the toxicity of this compound was quite severe and that relatively low concentrations needed to be used (Figure 19). We chose to use 0.1 µg/ml, in spite of some toxicity observed at this concentration, with the rationale that this compound would eventually be encapsulated and that systemic toxicity might no longer be a problem. Keeping in mind that approximately 40 % of the embryos will die due to toxicity, we still hoped to observe some therapeutic effect through fluorescence microscopy in the period before mortality became too high. Indeed, a therapeutic effect is seen for the group treated with 0.1 µg/ml TZ in combination with 320 µg/ml RIF (Figure 21), but whether or not it is significantly more than what was observed for the embryos treated with only 320 µg/ml RIF, is difficult to conclude. In this experiment, 320 µg/ml RIF had a much greater bactericidal effect than observed earlier (Figure 16 and 20). The reason for this is not clear; the bacterial load may have been affected due to some clogging of the needle during injection or it may be natural variability amongst the embryos. Either way, the effect was great enough as to determine the data not significantly different from the control group by a Log-rank test.

The same determination was made for the group treated with RIF and 0.01 µg/ml TZ, but I believe that this therapeutic effect is due to the RIF not the TZ. This is supported by the fact that there was no additional bactericidal effect observed in combination with RIF (Figure 21), and 0.01 µg/ml TZ did not have any bactericidal effect on its own (Figure 20 and 21). The same lack of bactericidal effect was observed for 0.1 µg/ml TZ as well. Therefore, in contrast to what has been reported, TZ did not under these circumstances show any bactericidal activity on its own, and it thereby makes it hard to conclude if there was any activity in combination with RIF as well.

These results are preliminary and this experiment needs to be repeated. Here and now it does not seem like TZ helps decrease the bacterial load significantly during infection, despite all the promising results that have been reported for this compound, but one must keep in mind that most experiments have been done in macrophage cell cultures relative to *in vivo* experiments. Therefore, more optimization of the system may be necessary. In addition, one can hypothesize that the reason for TZ's lack of activity could be the absence of efflux pump up-regulation all together. Other mechanisms of tolerance are known and have been shown in mycobacteria, e.g. rescue of the RNA polymerase from inhibition by RIF [125]. Obviously this is speculation as this is a phenomenon we know little about at the moment, and that requires extensive research.

6 Conclusions

The conclusions that can be drawn from this Master's thesis are:

- A procedure for obtaining small and uniformly distributed NPs was established.
- Protocols for pDNA-encapsulation and pDNA characterization were established.
- pDNA-encapsulation was not successful and thus, our particles could not yet be evaluated for therapeutic purposes.
- Treatment of *M.marinum*-infected zebrafish embryos with rifampicin induces tolerance towards the drug.
- The effect of TZ was evaluated by preliminary experiments and shown not to be as effective as we had expected.
- CFU enumeration needs to be further optimized.
- Gene expression analyses were inconclusive and therefore terminated.

7 Future perspectives

Nanoparticle preparation can be a lengthy process and the procedure needs to be continuously optimized until the desired properties are obtained. These properties include drug loading efficiency, size, surface modifications and etc. In the present work pDNA encapsulation was not successful due to reasons discussed earlier, therefore, new strategies need to be explored. One possibility, already used by some groups, could be to complex pDNA with polyethylene glycol (PEG). These nano-scale complexes have been shown to dissolve in selected organic solvents, such as DMSO [108]. Creating these complexes beforehand and dissolving them directly in the DMSO could be the answer to encapsulating pDNA with the nanoprecipitation method. Otherwise, I fear a different method of encapsulation, such as double emulsion, will have to be considered, despite the fact that there will be a risk of damage to the pDNA and that it will require a considerable amount of time and work.

After successful pDNA encapsulation, the NPs should be tested as therapeutic agents in BCG-infected macrophages and in *M.marinum*-infected zebrafish embryos. In addition, quantitative analyses of pDNA release from the NPs should be performed. The levels of gene expression should be evaluated using quantitative PCR and sub-cellular localization should be observed due to the GFP construct associated with the antimicrobial peptide. These studies will be important in establishing pDNA-NPs as therapeutic agents.

Preparation of particles with the optimal size was also not successful, but this can be used as an advantage. In addition to the work we are doing on TB therapy, we are also going to start exploring the possibilities of using NPs in cancer therapy as well. In that case, the protocol I established for the fabrication of these small NPs may be ideal for that purpose, since the particles need to travel through small capillaries to reach the cancerous sites of the human body.

One of the observations I made concerning RIF therapy was the same as Adams et al. 2011 [119]; some bacteria develop tolerance and persist during treatment. On the other hand, I did not obtain the same results concerning treatment with the MEC, 320 µg/ml, or the degree of toxicity observed when using a higher concentration of RIF (640 µg/ml). Due to these differences I would advise that more consistent data need to be collected in the form of repetition, and that quantitative analyses of RIF concentration inside treated embryos, in the form of high-performance liquid chromatography (HPLC), should be considered.

In addition to RIF, disappointing results were also obtained for TZ. TZ is reported to have considerable bactericidal activity against *M.tb* on its own and in combination with antibiotics. These effects were not observed in the preliminary experiment performed in this thesis' work, but as this was preliminary, the experiment should be repeated. There is some promise for TZ in our group since my colleague Raja Kalluru has recently shown that TZ free in solution, in conjunction with RIF-NPs is able to significantly improve the killing of BCG in mouse primary macrophages relative to cells treated with only RIF-NP. Efforts are now ongoing in the group to encapsulate TZ in order to test some of the hypotheses discussed in this thesis.

8 Appendix

8.1 Calculations

Rifampicin concentrations:

- Calculations for 100 µg/ml and 320 µg/ml are for a total volume of 90 ml (approx. 3 days worth of solution).

100 µg/ml: in 100 ml embryo water 10 mg RIF would have to be added to make a 100 µg/ml solution. 90 ml/100 ml = 0.9, this factor is used to calculate the amount of RIF needed in 90 ml embryo water: 10 mg RIF x 0.9 = **9 mg** RIF

RIF is dissolved in 1 % DMSO, here **0.9 ml**

0.9 ml RIF-DMSO solution is added to 90 ml – 0.9 ml = **89.1 ml** embryo water.

320 µg/ml: to make 100 ml of a 320 µg/ml solution one needs 32 mg.
As above, 32 mg RIF x 0.9 = **28.8 mg** RIF in 0.9 ml DMSO and subsequently 89.1 ml embryo water.

- The total volume for 500 µg/ml and 640 µg/ml solutions is 180 ml. The solutions are double because of the control groups.

500 µg/ml: for 100 ml of a 500 µg/ml solution one needs 50 mg.
The factor for calculation is now, 180 ml/100 ml = 1.8.
50 mg RIF x 1.8 = **90 mg** RIF in **1.8 ml** DMSO (1 % of total volume)

1.8 ml RIF-DMSO is added to 180 ml – 1.8 ml = **178.2 ml** embryo water.

640 µg/ml: to make 100 ml of a 640 µg/ml solution one needs 64 mg.
64 mg RIF x 1.8 = **115.2 mg** RIF in 1.8 ml DMSO and subsequently 178.2 ml embryo water.

8.2 Solutions

The following recipes are taken from Cosma et al. 2006 [115].

Embryo water:

1.0 ml Hanks' stock solution #1
0.1 ml Hanks' stock solution #2
1.0 ml Hanks' stock solution #4
95.9 ml H_2O
1.0 ml Hanks' stock solution #5
1.0 ml Hanks' stock solution #6

Adjust pH to 7.2, filter sterilize and store indefinitely at 4°C.

Hanks' stock solutions:

Stock #1: 8.0 g NaCl
0.4 g KCl
100 ml H_2O

Stock #2: 0.358 g Na_2HPO_4 anhydrous
0.6 g KH_2PO_4
100 ml H_2O

Stock #4: 0.72 g $CaCl_2$
50 ml H_2O

Stock #5: 1.23 g $MgSO_4 \cdot 7H_2O$
50 ml H_2O

Stock #6: 0.35 g $NaHCO_3$
10 ml H_2O

All solutions can be stored indefinitely at 4°C.

***M. marinum* freezing medium:**

This recipe is taken from Gao et al. 2005 [63].

Add the following components to 140 ml H_2O with constant stirring at room temperature and continue stirring for 10 min:
60 ml glycerol
1 ml 10 (v/v) Tween 80
Pass through a 0.22-µm filter to sterilize
Store up to three months at 4°C

9 References

1. http://www.who.int/tb/publications/2011/factsheet_tb_2011.pdf
2. Lillebaek, T., et al., *Molecular evidence of endogenous reactivation of Mycobacterium tuberculosis after 33 years of latent infection.* J Infect Dis, 2002. **185**(3): p. 401-4.
3. Russell, D.G., *Mycobacterium tuberculosis: here today, and here tomorrow.* Nature reviews. Molecular cell biology, 2001. **2**(8): p. 569-77.
4. http://www.who.int/tb/challenges/mdr/factsheet_mdr_progress_march2011.pdf
5. Sharma, S. and A. Singh, *Phenothiazines as anti-tubercular agents: mechanistic insights and clinical implications.* Expert opinion on investigational drugs, 2011. **20**(12): p. 1665-76.
6. Russell, D.G., C.E. Barry, 3rd, and J.L. Flynn, *Tuberculosis: what we don't know can, and does, hurt us.* Science, 2010. **328**(5980): p. 852-6.
7. Russell, D.G., H.C. Mwandumba, and E.E. Rhoades, *Mycobacterium and the coat of many lipids.* J Cell Biol, 2002. **158**(3): p. 421-6.
8. Vergne, I., et al., *Cell biology of mycobacterium tuberculosis phagosome.* Annu Rev Cell Dev Biol, 2004. **20**: p. 367-94.
9. Griffiths, G., et al., *Nanobead-based interventions for the treatment and prevention of tuberculosis.* Nat Rev Microbiol, 2010. **8**(11): p. 827-34.
10. Via, L.E., et al., *Arrest of mycobacterial phagosome maturation is caused by a block in vesicle fusion between stages controlled by rab5 and rab7.* The Journal of biological chemistry, 1997. **272**(20): p. 13326-31.
11. Russell, D.G., *Who puts the tubercle in tuberculosis?* Nat Rev Microbiol, 2007. **5**(1): p. 39-47.
12. van der Wel, N., et al., *M. tuberculosis and M. leprae translocate from the phagolysosome to the cytosol in myeloid cells.* Cell, 2007. **129**(7): p. 1287-98.
13. Simeone, R., et al., *Phagosomal rupture by Mycobacterium tuberculosis results in toxicity and host cell death.* PLoS pathogens, 2012. **8**(2): p. e1002507.
14. Jordao, L., et al., *On the killing of mycobacteria by macrophages.* Cellular microbiology, 2008. **10**(2): p. 529-48.
15. Laube, D.M., et al., *Antimicrobial peptides in the airway.* Current topics in microbiology and immunology, 2006. **306**: p. 153-82.
16. Marr, A.K., W.J. Gooderham, and R.E.W. Hancock, *Antibacterial peptides for therapeutic use: obstacles and realistic outlook.* Current Opinion in Pharmacology, 2006. **6**(5): p. 468-472.
17. Ganz, T., *Defensins: antimicrobial peptides of innate immunity.* Nature reviews. Immunology, 2003. **3**(9): p. 710-20.
18. Jena, P., et al., *Membrane-active antimicrobial peptides and human placental lysosomal extracts are highly active against mycobacteria.* Peptides, 2011. **32**(5): p. 881-7.
19. Agerberth, B., et al., *The human antimicrobial and chemotactic peptides LL-37 and alpha-defensins are expressed by specific lymphocyte and monocyte populations.* Blood, 2000. **96**(9): p. 3086-93.
20. Ganz, T., et al., *Defensins. Natural peptide antibiotics of human neutrophils.* The Journal of clinical investigation, 1985. **76**(4): p. 1427-35.
21. Sharma, S. and G. Khuller, *DNA as the intracellular secondary target for antibacterial action of human neutrophil peptide-I against Mycobacterium tuberculosis H37Ra.* Current microbiology, 2001. **43**(1): p. 74-6.

22. Lehrer, R.I., A.K. Lichtenstein, and T. Ganz, *Defensins: antimicrobial and cytotoxic peptides of mammalian cells.* Annual review of immunology, 1993. **11**: p. 105-28.
23. Mendez-Samperio, P., *Role of antimicrobial peptides in host defense against mycobacterial infections.* Peptides, 2008. **29**(10): p. 1836-41.
24. Ashitani, J., et al., *Elevated levels of alpha-defensins in plasma and BAL fluid of patients with active pulmonary tuberculosis.* Chest, 2002. **121**(2): p. 519-26.
25. Ogata, K., et al., *Activity of defensins from human neutrophilic granulocytes against Mycobacterium avium-Mycobacterium intracellulare.* Infection and immunity, 1992. **60**(11): p. 4720-5.
26. Miyakawa, Y., et al., *In vitro activity of the antimicrobial peptides human and rabbit defensins and porcine leukocyte protegrin against Mycobacterium tuberculosis.* Infection and immunity, 1996. **64**(3): p. 926-32.
27. Sharma, S., I. Verma, and G.K. Khuller, *Antibacterial activity of human neutrophil peptide-1 against Mycobacterium tuberculosis H37Rv: in vitro and ex vivo study.* The European respiratory journal : official journal of the European Society for Clinical Respiratory Physiology, 2000. **16**(1): p. 112-7.
28. Sharma, S., I. Verma, and G.K. Khuller, *Therapeutic potential of human neutrophil peptide 1 against experimental tuberculosis.* Antimicrobial agents and chemotherapy, 2001. **45**(2): p. 639-40.
29. Fattorini, L., et al., *In vitro activity of protegrin-1 and beta-defensin-1, alone and in combination with isoniazid, against Mycobacterium tuberculosis.* Peptides, 2004. **25**(7): p. 1075-7.
30. Rivas-Santiago, B., et al., *Human {beta}-defensin 2 is expressed and associated with Mycobacterium tuberculosis during infection of human alveolar epithelial cells.* Infection and immunity, 2005. **73**(8): p. 4505-11.
31. Kisich, K.O., et al., *Antimycobacterial agent based on mRNA encoding human beta-defensin 2 enables primary macrophages to restrict growth of Mycobacterium tuberculosis.* Infection and immunity, 2001. **69**(4): p. 2692-9.
32. Larrick, J.W., et al., *Human CAP18: a novel antimicrobial lipopolysaccharide-binding protein.* Infection and immunity, 1995. **63**(4): p. 1291-7.
33. Bals, R., et al., *The peptide antibiotic LL-37/hCAP-18 is expressed in epithelia of the human lung where it has broad antimicrobial activity at the airway surface.* Proceedings of the National Academy of Sciences of the United States of America, 1998. **95**(16): p. 9541-6.
34. Dürr, U.H.N., U.S. Sudheendra, and A. Ramamoorthy, *LL-37, the only human member of the cathelicidin family of antimicrobial peptides.* Biochimica et Biophysica Acta (BBA) - Biomembranes, 2006. **1758**(9): p. 1408-1425.
35. Rivas-Santiago, B., et al., *Expression of Cathelicidin LL-37 during Mycobacterium tuberculosis Infection in Human Alveolar Macrophages, Monocytes, Neutrophils, and Epithelial Cells.* Infection and Immunity, 2008. **76**(3): p. 935-941.
36. Liu, P.T., et al., *Toll-Like Receptor Triggering of a Vitamin D-Mediated Human Antimicrobial Response.* Science, 2006. **311**(5768): p. 1770-1773.
37. Andersson, M., et al., *NK-lysin, a novel effector peptide of cytotoxic T and NK cells. Structure and cDNA cloning of the porcine form, induction by interleukin 2, antibacterial and antitumour activity.* The EMBO journal, 1995. **14**(8): p. 1615-25.
38. Andreu, D., et al., *Identification of an anti-mycobacterial domain in NK-lysin and granulysin.* The Biochemical journal, 1999. **344 Pt 3**: p. 845-9.
39. Fedders, H., et al., *An exceptional salt-tolerant antimicrobial peptide derived from a novel gene family of haemocytes of the marine invertebrate Ciona intestinalis.* The Biochemical journal, 2008. **416**(1): p. 65-75.

40. Fedders, H., R. Podschun, and M. Leippe, *The antimicrobial peptide Ci-MAM-A24 is highly active against multidrug-resistant and anaerobic bacteria pathogenic for humans.* International Journal of Antimicrobial Agents, 2010. **36**(3): p. 264-266.
41. Blumberg, H.M.e.a., *American Thoracic Society/Centers for Disease Control and Prevention/Infectious Diseases Society of America.* American Journal of Respiratory and Critical Care Medicine, 2003. **167**(4): p. 603-662.
42. Nachega, J.B. and R.E. Chaisson, *Tuberculosis drug resistance: a global threat.* Clinical infectious diseases : an official publication of the Infectious Diseases Society of America, 2003. **36**(Suppl 1): p. S24-30.
43. Sensi, P., *History of the development of rifampin.* Reviews of infectious diseases, 1983. **5 Suppl 3**: p. S402-6.
44. Somoskovi, A., L. Parsons, and M. Salfinger, *The molecular basis of resistance to isoniazid, rifampin, and pyrazinamide in Mycobacterium tuberculosis.* Respiratory Research, 2001. **2**(3): p. 164 - 168.
45. Ellard, G.A. and P.B. Fourie, *Rifampicin bioavailability: a review of its pharmacology and the chemotherapeutic necessity for ensuring optimal absorption.* The international journal of tuberculosis and lung disease : the official journal of the International Union against Tuberculosis and Lung Disease, 1999. **3**(11 Suppl 3): p. S301-8; discussion S317-21.
46. Tostmann, A., et al., *Antituberculosis drug-induced hepatotoxicity: concise up-to-date review.* Journal of gastroenterology and hepatology, 2008. **23**(2): p. 192-202.
47. Bettencourt, M.V., S. Bosne-David, and L. Amaral, *Comparative in vitro activity of phenothiazines against multidrug-resistant Mycobacterium tuberculosis.* International Journal of Antimicrobial Agents, 2000. **16**(1): p. 69-71.
48. Amaral, L. and M. Viveiros, *Why thioridazine in combination with antibiotics cures extensively drug-resistant Mycobacterium tuberculosis infections.* International Journal of Antimicrobial Agents, 2012. **39**(5): p. 376-380.
49. Ordway, D., et al., *Clinical concentrations of thioridazine kill intracellular multidrug-resistant Mycobacterium tuberculosis.* Antimicrobial agents and chemotherapy, 2003. **47**(3): p. 917-22.
50. Crowle, A.J., G.S. Douvas, and M.H. May, *Chlorpromazine: a drug potentially useful for treating mycobacterial infections.* Chemotherapy, 1992. **38**(6): p. 410-9.
51. Amaral, L. and J.E. Kristiansen, *Phenothiazines: an alternative to conventional therapy for the initial management of suspected multidrug resistant tuberculosis. A call for studies.* International Journal of Antimicrobial Agents, 2000. **14**(3): p. 173-6.
52. van Soolingen, D., et al., *The antipsychotic thioridazine shows promising therapeutic activity in a mouse model of multidrug-resistant tuberculosis.* PloS one, 2010. **5**(9).
53. Hamilton, F., *An account of the fishes found in the river Ganges and its branches / by Francis Hamilton, (formerly Buchanan,) ...; With a volume of plates in royal quarto*. Vol. Text. 1822, Edinburgh :: Printed for A. Constable and company; [etc., etc.].
54. Sullivan, C. and C.H. Kim, *Zebrafish as a model for infectious disease and immune function.* Fish Shellfish Immunol, 2008. **25**(4): p. 341-50.
55. Grunwald, D.J. and J.S. Eisen, *Headwaters of the zebrafish -- emergence of a new model vertebrate.* Nat Rev Genet, 2002. **3**(9): p. 717-24.
56. Meijer, A.H. and H.P. Spaink, *Host-Pathogen Interactions Made Transparent with the Zebrafish Model.* Current Drug Targets, 2011. **12**(7): p. 1000-1017.
57. Lister, J.A., et al., *nacre encodes a zebrafish microphthalmia-related protein that regulates neural-crest-derived pigment cell fate.* Development, 1999. **126**(17): p. 3757-67.

58. Shestopalov, I.A. and J.K. Chen, *Oligonucleotide-based tools for studying zebrafish development.* Zebrafish, 2010. **7**(1): p. 31-40.
59. Bowman, T.V. and L.I. Zon, *Swimming into the future of drug discovery: in vivo chemical screens in zebrafish.* ACS chemical biology, 2010. **5**(2): p. 159-61.
60. Lam, S.H., et al., *Development and maturation of the immune system in zebrafish, Danio rerio: a gene expression profiling, in situ hybridization and immunological study.* Developmental and comparative immunology, 2004. **28**(1): p. 9-28.
61. Davis, J.M., et al., *Real-time visualization of mycobacterium-macrophage interactions leading to initiation of granuloma formation in zebrafish embryos.* Immunity, 2002. **17**(6): p. 693-702.
62. Madigan M.T., Martinko J.M., Dunlap P.V., and Clark D.P., Brock Biology of Microorganisms, Pearson education
63. Gao, L.Y. and J. Manoranjan, *Laboratory maintenance of Mycobacterium marinum.* Current protocols in microbiology, 2005. **Chapter 10**: p. Unit 10B 1.
64. Barker, L.P., et al., *Differential trafficking of live and dead Mycobacterium marinum organisms in macrophages.* Infection and immunity, 1997. **65**(4): p. 1497-504.
65. Tonjum, T., et al., *Differentiation of Mycobacterium ulcerans, M. marinum, and M. haemophilum: mapping of their relationships to M. tuberculosis by fatty acid profile analysis, DNA-DNA hybridization, and 16S rRNA gene sequence analysis.* J Clin Microbiol, 1998. **36**(4): p. 918-25.
66. Swaim, L.E., et al., *Mycobacterium marinum infection of adult zebrafish causes caseating granulomatous tuberculosis and is moderated by adaptive immunity.* Infect Immun, 2006. **74**(11): p. 6108-17.
67. Tobin, D.M. and L. Ramakrishnan, *Comparative pathogenesis of Mycobacterium marinum and Mycobacterium tuberculosis.* Cell Microbiol, 2008. **10**(5): p. 1027-39.
68. Lesley, R. and L. Ramakrishnan, *Insights into early mycobacterial pathogenesis from the zebrafish.* Curr Opin Microbiol, 2008. **11**(3): p. 277-83.
69. Trede, N.S.L., D. M.; Traver, D.; Look, A. T.; Zon, L. I., *The Use of Zebrafish to Understand Immunity.* Immunity, 2004. **20**.
70. Meeker, N.D. and N.S. Trede, *Immunology and zebrafish: spawning new models of human disease.* Developmental and comparative immunology, 2008. **32**(7): p. 745-57.
71. Meijer, A.H., et al., *Expression analysis of the Toll-like receptor and TIR domain adaptor families of zebrafish.* Molecular immunology, 2004. **40**(11): p. 773-83.
72. Petrie-Hanson, L., C. Hohn, and L. Hanson, *Characterization of rag1 mutant zebrafish leukocytes.* BMC immunology, 2009. **10**: p. 8.
73. Zou, J., et al., *Discovery of multiple beta-defensin like homologues in teleost fish.* Molecular immunology, 2007. **44**(4): p. 638-47.
74. Flynn, J.L., *Lessons from experimental Mycobacterium tuberculosis infections.* Microbes and infection / Institut Pasteur, 2006. **8**(4): p. 1179-88.
75. Ramakrishnan, L., et al., *Mycobacterium marinum causes both long-term subclinical infection and acute disease in the leopard frog (Rana pipiens).* Infection and immunity, 1997. **65**(2): p. 767-73.
76. Bouley, D.M., et al., *Dynamic nature of host-pathogen interactions in Mycobacterium marinum granulomas.* Infect Immun, 2001. **69**(12): p. 7820-31.
77. Takahashi, K., *Development and Differentiation of Macrophages and Related Cells: Historical Review and Current Concepts.* Journal of Clinical and Experimental Hematopathology, 2001. **41**.
78. Volkman, H.E., et al., *Tuberculous granuloma formation is enhanced by a mycobacterium virulence determinant.* PLoS Biol, 2004. **2**(11): p. e367.

79. Guinn, K.M., et al., *Individual RD1-region genes are required for export of ESAT-6/CFP-10 and for virulence of Mycobacterium tuberculosis.* Molecular microbiology, 2004. **51**(2): p. 359-70.
80. Cosma, C.L., O. Humbert, and L. Ramakrishnan, *Superinfecting mycobacteria home to established tuberculous granulomas.* Nat Immunol, 2004. **5**(8): p. 828-35.
81. Clay, H., et al., *Dichotomous role of the macrophage in early Mycobacterium marinum infection of the zebrafish.* Cell Host Microbe, 2007. **2**(1): p. 29-39.
82. Ramakrishnan, L., *Revisiting the role of the granuloma in tuberculosis.* Nature reviews. Immunology, 2012. **12**(5): p. 352-66.
83. Davis, J.M. and L. Ramakrishnan, *The role of the granuloma in expansion and dissemination of early tuberculous infection.* Cell, 2009. **136**(1): p. 37-49.
84. Couvreur, P. and C. Vauthier, *Nanotechnology: intelligent design to treat complex disease.* Pharm Res, 2006. **23**(7): p. 1417-50.
85. Shive, M.S. and J.M. Anderson, *Biodegradation and biocompatibility of PLA and PLGA microspheres.* Advanced drug delivery reviews, 1997. **28**(1): p. 5-24.
86. Hans, M.L. and A.M. Lowman, *Biodegradable nanoparticles for drug delivery and targeting.* Current Opinion in Solid State and Materials Science, 2002. **6**(4): p. 319-327.
87. Armstead, A.L. and B. Li, *Nanomedicine as an emerging approach against intracellular pathogens.* International journal of nanomedicine, 2011. **6**: p. 3281-93.
88. Bilati, U., E. Allemann, and E. Doelker, *Nanoprecipitation versus emulsion-based techniques for the encapsulation of proteins into biodegradable nanoparticles and process-related stability issues.* AAPS PharmSciTech, 2005. **6**(4): p. E594-604.
89. Almouazen, E., et al., *Development of a nanoparticle-based system for the delivery of retinoic acid into macrophages.* International Journal of Pharmaceutics, 2012. **430**(1–2): p. 207-215.
90. Panyam, J. and V. Labhasetwar, *Biodegradable nanoparticles for drug and gene delivery to cells and tissue.* Advanced drug delivery reviews, 2003. **55**(3): p. 329-47.
91. Dong, L., et al., *Targeting delivery oligonucleotide into macrophages by cationic polysaccharide from Bletilla striata successfully inhibited the expression of TNF-α.* Journal of Controlled Release, 2009. **134**(3): p. 214-220.
92. Sharma, A., S. Sharma, and G.K. Khuller, *Lectin-functionalized poly (lactide-co-glycolide) nanoparticles as oral/aerosolized antitubercular drug carriers for treatment of tuberculosis.* J Antimicrob Chemother, 2004. **54**(4): p. 761-6.
93. Steele-Mortimer, O., *The Salmonella-containing vacuole: moving with the times.* Current opinion in microbiology, 2008. **11**(1): p. 38-45.
94. Portnoy, D.A. and S. Jones, *The cell biology of Listeria monocytogenes infection (escape from a vacuole).* Annals of the New York Academy of Sciences, 1994. **730**: p. 15-25.
95. Hirota, K., et al., *Delivery of rifampicin–PLGA microspheres into alveolar macrophages is promising for treatment of tuberculosis.* Journal of Controlled Release, 2010. **142**(3): p. 339-346.
96. Pandey, R., S. Sharma, and G.K. Khuller, *Chemotherapeutic efficacy of nanoparticle encapsulated antitubercular drugs.* Drug Deliv, 2006. **13**(4): p. 287-94.
97. Pandey, R., et al., *Nanoparticle encapsulated antitubercular drugs as a potential oral drug delivery system against murine tuberculosis.* Tuberculosis (Edinb), 2003. **83**(6): p. 373-8.
98. Sharma, A., et al., *Chemotherapeutic efficacy of poly (DL-lactide-co-glycolide) nanoparticle encapsulated antitubercular drugs at sub-therapeutic dose against experimental tuberculosis.* Int J Antimicrob Agents, 2004. **24**(6): p. 599-604.

99. Pandey, R., et al., *Poly (DL-lactide-co-glycolide) nanoparticle-based inhalable sustained drug delivery system for experimental tuberculosis.* J Antimicrob Chemother, 2003. **52**(6): p. 981-6.
100. Bowman, K. and K.W. Leong, *Chitosan nanoparticles for oral drug and gene delivery.* International journal of nanomedicine, 2006. **1**(2): p. 117-28.
101. Luten, J., et al., *Biodegradable polymers as non-viral carriers for plasmid DNA delivery.* Journal of controlled release : official journal of the Controlled Release Society, 2008. **126**(2): p. 97-110.
102. Ravi Kumar, M.N., U. Bakowsky, and C.M. Lehr, *Preparation and characterization of cationic PLGA nanospheres as DNA carriers.* Biomaterials, 2004. **25**(10): p. 1771-7.
103. Mok, H. and T.G. Park, *Direct plasmid DNA encapsulation within PLGA nanospheres by single oil-in-water emulsion method.* European journal of pharmaceutics and biopharmaceutics : official journal of Arbeitsgemeinschaft fur Pharmazeutische Verfahrenstechnik e.V, 2008. **68**(1): p. 105-11.
104. Wang, D., et al., *Encapsulation of plasmid DNA in biodegradable poly(D, L-lactic-co-glycolic acid) microspheres as a novel approach for immunogene delivery.* Journal of controlled release : official journal of the Controlled Release Society, 1999. **57**(1): p. 9-18.
105. Mao, H.Q., et al., *Chitosan-DNA nanoparticles as gene carriers: synthesis, characterization and transfection efficiency.* Journal of controlled release : official journal of the Controlled Release Society, 2001. **70**(3): p. 399-421.
106. Tse, M.T., C. Blatchford, and H. Oya Alpar, *Evaluation of different buffers on plasmid DNA encapsulation into PLGA microparticles.* International journal of pharmaceutics, 2009. **370**(1-2): p. 33-40.
107. Zhang, X.Q., J. Intra, and A.K. Salem, *Comparative study of poly (lactic-co-glycolic acid)-poly ethyleneimine-plasmid DNA microparticles prepared using double emulsion methods.* Journal of microencapsulation, 2008. **25**(1): p. 1-12.
108. Mok, H. and T.G. Park, *PEG-assisted DNA solubilization in organic solvents for preparing cytosol specifically degradable PEG/DNA nanogels.* Bioconjugate chemistry, 2006. **17**(6): p. 1369-72.
109. Niu, X., et al., *Modified nanoprecipitation method to fabricate DNA-loaded PLGA nanoparticles.* Drug development and industrial pharmacy, 2009. **35**(11): p. 1375-83.
110. Fessi, H., et al., *Nanocapsule formation by interfacial polymer deposition following solvent displacement.* International Journal of Pharmaceutics, 1989. **55**(1): p. R1-R4.
111. Wattiaux, R., et al., *Endosomes, lysosomes: their implication in gene transfer.* Advanced drug delivery reviews, 2000. **41**(2): p. 201-8.
112. Panyam, J., et al., *Rapid endo-lysosomal escape of poly(DL-lactide-co-glycolide) nanoparticles: implications for drug and gene delivery.* FASEB journal : official publication of the Federation of American Societies for Experimental Biology, 2002. **16**(10): p. 1217-26.
113. Boussif, O., et al., *A versatile vector for gene and oligonucleotide transfer into cells in culture and in vivo: polyethylenimine.* Proceedings of the National Academy of Sciences of the United States of America, 1995. **92**(16): p. 7297-301.
114. Tang, M.X. and F.C. Szoka, *The influence of polymer structure on the interactions of cationic polymers with DNA and morphology of the resulting complexes.* Gene therapy, 1997. **4**(8): p. 823-32.
115. Cosma, C.L., et al., *Zebrafish and frog models of Mycobacterium marinum infection.* Curr Protoc Microbiol, 2006. **Chapter 10**: p. Unit 10B 2.

116. Rosen, J.N., M.F. Sweeney, and J.D. Mably, *Microinjection of Zebrafish Embryos to Analyze Gene Function.* J Vis Exp, 2009(25): p. e1115.
117. Kavaliauskis, A., *Towards the development of nanobead vaccines against salmon pathogens: establishment of cold-water fish infection models*, 2011, A. Kavaliauskis: Oslo. p. VIII, 72 s.
118. Gupta, T. and M.C. Mullins, *Dissection of Organs from the Adult Zebrafish.* J Vis Exp, 2010(37): p. e1717.
119. Adams, K.N., et al., *Drug Tolerance in Replicating Mycobacteria Mediated by a Macrophage-Induced Efflux Mechanism.* Cell, 2011.
120. Bilati, U., E. Allémann, and E. Doelker, *Development of a nanoprecipitation method intended for the entrapment of hydrophilic drugs into nanoparticles.* European Journal of Pharmaceutical Sciences, 2005. **24**(1): p. 67-75.
121. Aubry, A., et al., *Antibiotic susceptibility pattern of Mycobacterium marinum.* Antimicrobial agents and chemotherapy, 2000. **44**(11): p. 3133-6.
122. Wolinsky, E., *Mycobacterial Diseases Other than Tuberculosis.* Clinical Infectious Diseases, 1992. **15**(1): p. 1-10.
123. Cosma, C.L., et al., *Mycobacterium marinum Erp is a virulence determinant required for cell wall integrity and intracellular survival.* Infect Immun, 2006. **74**(6): p. 3125-33.
124. Donald, P.R. and A.H. Diacon, *The early bactericidal activity of anti-tuberculosis drugs: a literature review.* Tuberculosis, 2008. **88 Suppl 1**: p. S75-83.
125. Dey, A., A.K. Verma, and D. Chatterji, *Molecular insights into the mechanism of phenotypic tolerance to rifampicin conferred on mycobacterial RNA polymerase by MsRbpA.* Microbiology, 2011. **157**(7): p. 2056-2071.